Journal Pre-proof

The late Paleocene-Eocene interval of the Magallanes-Austral Basin (Chile-Argentina): Palynostratigraphy, paleoclimate and geochemical data

Mirta E. Quattrocchio, Pablo E. Diaz, Luis S. Agüero

PII: S0895-9811(23)00518-7

DOI: https://doi.org/10.1016/j.jsames.2023.104706

Reference: SAMES 104706

To appear in: *Journal of South American Earth Sciences*

Received Date: 26 September 2023

Revised Date: 16 November 2023

Accepted Date: 17 November 2023

Please cite this article as: Quattrocchio, M.E., Diaz, P.E., Agüero, L.S., The late Paleocene-Eocene interval of the Magallanes-Austral Basin (Chile-Argentina): Palynostratigraphy, paleoclimate and geochemical data, *Journal of South American Earth Sciences* (2023), doi: https://doi.org/10.1016/j.jsames.2023.104706.

The late Paleocene-Eocene interval of the Magallanes-Austral basin (Chile-Argentina): palynostratigraphy, paleoclimate and geochemical data

Mirta E. Quattrocchio[a], Pablo E. Diaz[b], Luis S. Agüero[b]

[a] *Departamento de Geología, Universidad Nacional del Sur*

[b] *Instituto Geológico del Sur (INGEOSUR), Universidad Nacional del Sur-CONICET, Av. Alem 1253, Cuerpo B´, B8000ICN Bahía Blanca, Buenos Aires Province, Argentina*

Corresponding author: Mirta E. Quattrocchio (*E-mail address*: mquattro@criba.edu.ar)

Keywords. Paleocene-Eocene transition. Magallanes-Austral basin. Palynostratigraphy. Paleoenvironment. Geochemistry.

ABSTRACT

The Magallanes-Austral Foreland Basin preserves an important record of orogenesis and landscape evolution in the Patagonian Andes of Chile and Argentina. This paper evaluates the comparison between the thick Paleogene sequences in the Chilean Peninsula Brunswick (Chorrillo Chico and Agua Fresca formations) and the reduced Paleogene sequence (La Barca Formation) in the Punta Ainol locality, Argentina, by taking account of palynological and geochemical analyses. Warm and humid subtropical conditions (Subtropical Gondwanic Paleoflora) are inferred for the late Paleocene-Eocene interval studied. A new record of Lactoridaceae in the La Barca Formation expanded the known fossil range of this family in Patagonia. During the late Paleocene the Chorrillo Chico and La Barca formations would have been deposited mainly from hyperpycnal flows and this accumulation process continued until the Lutenian in the La Barca Formation. A relative

rise in the sea level in the early Eocene would be recognized in both sections. In the middle Eocene a relative fall in the sea level would have occurred with increased terrigenous influx. The rate of sedimentation was similar in both sections during the Thanetian and Ypresian intervals according to the ages assigned by biostratigraphy, suggesting that the sedimentation rate would have been controlled mainly by relative changes in sea level during the Paleocene-Eocene transition. Paleoenvironmental changes during the Paleocene-Eocene transition were characterized at the La Barca Formation of the Punta Ainol section, considering the new geochemical and palynological data provided in this contribution.

1. Introduction

The Magallanes-Austral Foreland Basin preserves an important record of orogenesis and landscape evolution in the Patagonian Andes of Chile and Argentina (Biddle et al., 1986; Malumián, 1999).

A Carbon Isotope Excursion (CIE) together with *Apectodinium*-dominated dinoflagellate cyst assemblages are primary criteria worldwide for the definition of the Paleocene-Eocene (P/E) boundary (Bujak and Brinkhuis, 1998; Crouch, 2001; Crouch et al., 2003; Cybulska and Rubinkiewicz, 2020). Sluijs et al. (2011) have shown the global dominance of *Apectodinium* prior to the CIE (Quattrocchio, 2020). *Apectodinium* first evolved at low latitudes during the middle Paleocene (Prevot et al., 1979; Brinkhuis et al., 1994) and appears to have migrated to middle and high latitudes during the late Paleocene due to global warming (Bujak and Brinkhuis, 1998).

The paleoenvironmental analysis of dinoflagellate cysts is key to understanding Paleogene paleoceanographic change and climate dynamics (Sluijs et al., 2005). In recent years, significant progress has been made in the integration of these microfossil

assemblages with geochemical, oceanographic, and physical reconstructions and several high-resolution records have been reported worldwide (Frieling and Sluijs 2018).

In particular, the Paleocene-Eocene boundary was a period of transient and intense global warming that had a profound effect on middle and high latitude biotas. A pronounced feature of the Paleocene-Eocene transition is that physical and geochemical changes affected both terrestrial and marine biota simultaneously (e.g., Crouch, 2001; Greenwood et al., 2003; Wilf et al., 2013; Woodburne et al., 2014).

Most of the data on organic, inorganic, and isotopic geochemical changes during the P/E transition come from Northern Hemisphere localities (Crouch, 2001; Crouch et al., 2003; Sluijs et al., 2011). Recognition of equivalent successions in the Southern Hemisphere is rare due to the land mass distribution and a comparatively short history of geological research. Detailed records of biotic and geochemical response during the Paleocene-Eocene transition from Southern Hemisphere localities can provide a greater insight into the mechanisms and causes of paleoenvironmental changes during this unique time interval. In this study, we address these issues by applying a palynological and geochemical approach, integrating the analysis of sporomorphs and dinoflagellate cysts with organic and inorganic chemostratigraphy of two expanded sedimentary successions, Punta Prat (Chorrillo Chico and Agua Fresca formations) and Punta Ainol (La Barca Formation) localities, in the Magallanes-Austral Basin (Fig. 1) during the Paleocene-Eocene transition. The aim of the combination of these techniques is to characterize the paleoclimatic variability and relative sea level fluctuations as drivers of the changes in both successions and to create a stratigraphic framework for the late Paleocene and Eocene in southern South America.

In this contribution, the associations of continental palynomorphs of the La Barca Formation in the Punta Ainol locality are documented for the first time. The first records

of paleoenviromental and paleoclimatic conditions were inferred from palynomorph data from the Punta Prat and Punta Ainol sections using additional published information on sporomorphs corresponding to the Chorrillo Chico and Agua Fresca formations (Carrillo Berumen et al., 2013). The dinoflagellate cyst assemblages from the Punta Prat section were published in Quattrocchio and Sarjeant (2003) and Quattrocchio (2009), and dinoflagellate cyst data from the La Barca Formation at the Punta Ainol locality were published in Quattrocchio (2021).

2. Geological setting and Palynostratigraphy

2.1. Geological setting

The Magallanes-Austral Basin (Chile-Argentina), which developed in the southern tip of South America, is related to the evolution of Cenozoic marine basins associated with the tectonically active margin of the Andes. During the Cenozoic, Patagonia was repeatedly inundated by the Atlantic and these marine transgression periods alternated with periods of non-marine sedimentation and erosion (Biddle et al., 1986; Malumián, 1999). The thickest marine outcrop is located in the western region; Bijl et al. (2021), and bibliography cited therein, gave a detailed chronostratigraphic framework for the sequences through dinoflagellate cyst biostratigraphy and radiometric dating of zircons.

The stratigraphic successions involved in the thrust-fold belt correspond to the Magallanes-Austral Foreland Basin and they have been divided into several unconformity-bounded sequences (Olivero and Malumián, 2008; Bijl et al., 2021), which record the kinematic evolution of the Fuegian Thrust-Fold Belt.

The sum of the thicknesses of the Chorrillo Chico and Agua Fresca formations at their type localities is approximately 3000 stratigraphic meters (Decat and Pomeyrol, 1931; Martinez-Pardo, 1971), deposited during the regressive-transgressive event that occurred

from the Paleocene to the Eocene (Malumián, 1999; Malumián et al., 2013) (Fig. 1.B). This event had only been recognized in the main depocenters, based on the study of planktonic and benthic foraminifera (Natland et al., 1974) and dinoflagellate cysts. It is well represented in the Punta Prat locality (53° 9' 50.594" S; 71° 34' 14.689" W - 53° 10' 4.148" S; 71° 33' 42.354" W, Fig. 1.B) in Chile (Quattrocchio and Sarjeant, 2003; Quattrocchio, 2009) located in the external thrust-fold belt (Torres Carbonell and Olivero, 2019).

Mainly for the Chorrillo Chico Formation, the lithofacies would correspond to hyperpycnal flows (Carrillo-Berumen et al., 2013), i.e., fluvial discharges originating in the continent with interstitial fresh water (extrabasinal turbidites type E) (Zavala, 2020).

At the type locality (Cabo Leticia), the La Barca Formation consists of a ~ 220m section with two members: a lower member LB1, composed of tuffaceous sandstones interbedded with carbonaceous siltstones; and an upper member LB2, composed of black mudstones (Olivero and Malumián, 2008; Quattrocchio, 2017) (Fig. 1.C).

At Punta Ainol, in the east of Tierra del Fuego Island (54° 35' 32.273" S; 65° 59' 42.450" W - 54° 35' 40.423" S; 65° 59' 56.098" W, Fig. 1.C), only LB2 (~120 m thick) is exposed in the external thrust-fold belt and it comprises predominant dark mudstones with siliceous sponge spicules, agglutinated foraminifera (Torres Carbonell et al., 2009; Cuciniello et al., 2017) and calcareous nannofossils (Bedoya Agudelo et al., 2018; Torres Carbonell and Olivero, 2019). The organic-rich mudstone samples from Punta Ainol contain calcareous nannofossils that correlate with other Paleocene-Eocene assemblages from the Southern Hemisphere (Bedoya Agudelo et al., 2018). Punta Ainol is a rocky outcrop, which is conspicuous at low tide, located between Cabo Jose and Cabo Leticia around the mouth of the Rodas stream (Torres Carbonell et al., 2009). According to Torres

Carbonell et al. (2009) the sequence of the La Barca Formation (LB2) is inverted and its base is not exposed.

The LB2 Member in Punta Ainol is interpreted to have been deposited by hyperpycnal density flows (Ronchi et al., 2015, Torres Carbonell and Olivero, 2019). This type of density flow typically transports large volumes of sediment and organic matter from proximal to deep-marine settings (Quattrocchio et al., 2018). The presence of *Impagidinium,* an oceanic taxon (Sluijs et al., 2005), could indicate the distality of the setting. A similar situation is observed in the Chorrillo Chico Formation (Carrillo-Berumen et al., 2013), with which the La Barca Formation (in part) is correlated (Malumián et al., 2013).

2.2 Palynostratigraphy

The entire assemblage and the stratigraphically significant species of the Chorrillo Chico and Agua Fresca formations is based on Quattrocchio and Sarjeant (2003) and Quattrocchio (2009), documented in Figure 2-3 and illustrated in Plate I. In the profiles, the first occurrence (FO) refers to the oldest, lowest or first occurrence of a taxon and the last occurrence (LO) to youngest, highest or last occurrence of a taxon.

The interval between PP5 and PP7 (Figure 2) suggests an age no younger than late Selandian due to the presence of *Palaeoperidinium pyrophorum* (68.20–59.20 Ma, Bijl et al., 2013).

In PP9 *Magallanesium macmurdoense* (*Spinidinium macmurdoense*) is recorded. This species has its First Appearance Datum (FAD) in the high latitudes of the Southern Hemisphere in the uppermost Chron 25 (57.0 Ma, Williams et al., 2004; 56.8 Ma, Bijl et al., 2013). *Deflandrea cygniformis,* present in PP10, has its FAD in the middle part of Chron 24 at 55.0 Ma in the Southern Hemisphere (Williams et al., 2004) and therefore probably reflects an age near the Paleocene/Eocene boundary.

In the Agua Fresca Formation (PP13), the FO of *Impagidinium cassiculum* (54.30–52.10 Ma, Bijl et al. 2013) indicates an early Eocene age. The FO of *Pyxidiniopsis delicata* in PP15, reflects the middle part of the early Eocene (*Kisselovia coleothrypta* Zone of Wilson, 1988). Additionally, the middle Eocene to middle Miocene marker *Lejeunecyta fallax* is recorded (PP19-PP20; PP26). *Alterbidinium distinctum* (PP23) has a Southern Hemisphere mid-latitude FAD in Chron 27, 37.0 Ma associated with the middle-late Eocene boundary (Williams et al., 2004). The *Achilleodinium biformoides* FAD (PP24-PP25), in equatorial latitudes, is within the latest Chron 13 (late Eocene, 33.7 Ma) according to Williams et al. (2004).

The absence of *Apectodinium* possibly indicates a hiatus at the Paleocene-Eocene boundary in the area (Quattrocchio, 2009). Biddle et al. (1986) interpreted the top of the Chorrillo Chico Formation as a possibly mid-Thanetian (late Paleocene) unconformity. This unconformity is apparently of regional extent and is present in southern South America and in the subsurface of the Magallanes and Malvinas-Falklands basins.

Based on Quattrocchio (2021), some significant dinoflagellate cyst biostratigraphic events are recognized in the Punta Ainol section (Figure 3) associated with *Apectodinium*. Throughout the studied section the FOs of *A. homomorphum* (FAD 58.8 Ma, LAD 48.3 Ma, Bijl et al., 2013) and *Impagidinium crassimuratum* (FAD 55.20 Ma, Bijl et al., 2013) are recorded at 49 m. The FO of *Impagidinium cassiculum* (54.30–52.10 Ma, Bijl et al. 2013) at 62 m and *Samlandia septata* at 71 m (FAD 53.3 Ma, LAD 51.8 Ma, Bijl et al., 2013) are also documented. Based on the presence of these taxa, an age no older than early Eocene is suggested for this part of the LB2 member of the La Barca Formation. *Cleistosphaeridium diversispinosum* (FAD 49.3 Ma, LAD 37.8 Ma, Bijl et al., 2013) is present at 77 m, its stratigraphic range extends from the late Ypresian to the Bartonian in the South Pacific Ocean (FO: 49.30 Ma, LO: 38.30 Ma according to Bijl et al., 2013).

The upper part of the section (88 m) is attributed to the Lutetian due to the presence of *Enneadocysta dictyostila* (FAD 47.9 Ma, LAD 33.2 Ma, Bijl et al., 2013). At 102 m only sporomorphs were recognized.

3. Material and methods

3.1. Palynology

Eighteen samples were studied from outcrop samples from the Punta Ainol locality. Physical and chemical extraction was carried out using standard palynological processing techniques (Volkheimer and Melendi, 1976), which involve treatment with hydrochloric and hydrofluoric acids. Nitric acid was used to produce a brief oxidation (two minutes or less). The residue was sieved through a 10µm mesh to concentrate the palynomorphs. All the specimens mentioned are stored in the collection of the Palynological Laboratory at Universidad Nacional del Sur, Bahía Blanca, Argentina.

The taxonomy of the dinoflagellate cyst species follows Williams et al., 2017. Age determinations are based on well-known First Appearance Datum (FAD) and Last Appearance Datum (LAD), especially for the Southern Hemisphere (Williams et al., 2004; Bijl et al., 2013).

In order to recognize paleoenvironmental trends in the palynomorph records, spore abundance and paleoecological preferences of each dinoflagellate cyst taxon were considered.

The paleoecological preferences considered are those of ecogroups or groups of dinoflagellate cysts (i.e., complexes of taxa that are closely related morphologically), widely applied in several studies (e.g., Brinkhuis, 1994; Powell et al., 1996; Lamolda and Mao, 1999; Pross and Brinkhuis, 2005; Sluijs et al., 2005; Frieling and Sluijs, 2018;

Steeman et al., 2020; Quattrocchio et al., 2021), and/or to paleoecological preferences well known in the literature (Table 4).

3.2. Geochemistry

Organic geochemical analyses were performed with a Rock-Eval 6 Pyro-Analyzer at the geochemical laboratory of Y-TEC (YPF Tecnología), Berisso, Buenos Aires, Argentina. Total organic carbon (TOC), total inorganic carbon (TIC) and hydrogen index (HI) were measured by a programmed Basic/Bulk-Rock open system Rock-Eval pyrolysis, according to Behar et al. (2001).

Inorganic geochemical analysis was performed with X-Ray Fluorescence (XRF) equipment at the sedimentary laboratory of Y-TEC, Berisso, Buenos Aires, Argentina. Twenty-six samples of sedimentary rocks were analyzed with a Thermo Scientific NITON XL3t XRF-Analyzer, using a gold anode tube with 50 kV voltage, 200 µA of current during 120 seconds, to obtain data for the following elements: Ti, Ca, Rb, Sr, Mn, Fe and P. Geochemical analysis focused mainly on elemental ratios to avoid misinterpretations due to possible dilution (e.g., carbonates, organic matter) (Löwemark et al., 2011).

Eight curves were performed for the Punta Prat and Punta Ainol sections (Figs. 2, 3, Supplementary data geochemistry) based on results from the pyrolysis analysis as TOC, TIC and HI, and according to elemental trends of Ca and P concentrations and Ti/Ca, Rb/Sr and Mn/Fe ratios. The amounts of organic matter were examined using a TOC (%) curve (Tribovillard et al., 2006). Furthermore, organic matter type was assessed using the HI curve (mg HC/g TOC) according to Peters (1986) and Exon et al. (2001). Calcite (CaCO3) concentration was estimated with TIC (%) and Ca (%) curves (Sageman and Lyons, 2004). The degree of weathering was evaluated using the Rb/Sr curve (Dasch, 1969; Chen et al., 1999; Buggle et al., 2011; Candel et al., 2020; Sue et al., 2022). Clastic

input was interpreted from the Ti/Ca curve fluctuations (Ingram et al., 2013). The P curve (ppm) was taken as a paleoproductivity proxy (Tribovillard et al., 2006) and the Mn/Fe curve was used as an indicator for paleo-redox conditions (Davison, 1993; Koinig et al., 2003; Burn and Palmer, 2014).

In addition, carbon isotope analyses from the Punta Prat section were performed at the Earth Sciences Department at Utrecht University, Utrecht, the Netherlands, with the aim to identify the CIE that characterized the PETM (Kennett and Stott, 1991; Koch et al., 1992; Schouten et al., 2007).

4. Results and discussion

4.1. Paleocommunities and paleoclimatic inferences

Sporomorph analysis at the Punta Ainol locality, La Barca Formation (Plate II), allowed the characterization of the paleofloristic and paleoclimatic scenario of the studied section during the late Paleocene-Eocene interval. The distribution charts of sporomorphs, the list of identified species and the botanical affinities are given in Table 1. It reflects a regional forest dominated by Araucariaceae, Nothofagaceae, Podocarpaceae and Proteaceae, accompanied by abundant ferns belonging to the Schizaeaceae, Polypodiaceae and Dicksoniaceae families, developed under a temperate to warm-temperate and humid climate. The species of *Nothofagidites* correspond to *N. fortispinulosus*, *N. rocaensis* and *N. saraensis*, which are similar to the *Nothofagus* "*Dombey*i type" and, among others, include the current *N. dombeyi* (Mirb.) Oerst. and *N. antarctica* (Forst.) Oerst. These two species are opposite ecologic indicators. The first corresponds to the evergreen forest and the second to the microtermic and deciduous forest. So, the paleoenviromental inferences with these morphospecies are limited (Quattrocchio et al., 2013 and bibliography cited therein), but high humidity conditions

are inferred due to the presence of *Phyllocladidites mawsonii* in the present association. This is compatible with the presence of the evergreen forest in the studied interval.

The pollen grains of *Phyllocladidites mawsonii* Cookson are very similar to that of *Lagarostrobus franklinii* (Hook) Quinn. *L. franklinii* is currently restricted to high-rainfall areas in western Tasmania, where the annual precipitation is up to 2,500 mm. Its habitat is banks of rivers and swampy flats up to 750 m.

Podocarpidites is associated with the living genus *Podocarpus*, which has a wide latitudinal distribution even recognized in mountainous areas of tropical regions (Barreda, 1996). Paleoclimatic estimation shows that this family has a mean annual temperature (MAT) of 17 °C and mean annual precipitation of 1,839.6 mm (Carvajal, 2013).

The frequent presence of gymnosperms suggests that the parent plants grow near to the site of deposition. Their anemophilous pollen grains (*Phyllocladidites*, *Podocarpidites* and *Microcachryidites*) characterize the regional input of palynomorphs in the depositional site.

The Araucariaceae community may have occupied ecotones associated with lowlands (García et al., 2006). Some authors even related them with coastal (Abbink, 1998) and/or swampy (Whitaker et al., 1992) communities. The morphological and structural features of their pollen grains suggest that they are not suitable for transport over large distances or for eolian dispersion. The presence of high proportions of araucariacean pollen grains may be related to forests of altitude or to relatively lower areas where pollen was transported principally by fluvial currents (Martínez et al., 1996). Paleoclimatic estimation shows that this family has a mean annual temperature of 17 °C and mean annual precipitation of 1,839.6 mm (Carvajal, 2013).

The Lactoridaceae is a monotypic shrub family confined to the Juan Fernandez Islands, located off the coast of Chile, which is found in wet montane forest above 500 m (Zavada and Benson, 1987).

The presence of Rubiaceae *Randia* (*Canthiumidites* aff. *C. bellus*) was recorded, which is a Neotropical genus (Salas, 2021) ranging from c. 30° N to 30° S. It is represented by shrubs, trees, and lianas from sea level to 3,300 m in the deciduous and evergreen forests (Gustafsson, 2000).

Pandanaceae (*Pandanus*) can also be recognized, associated with lowland environments. They grow along seacoasts and in marshy places in forests of tropical and subtropical regions (Petriella and Archangelsky, 1975).

Volkheimer et al. (2007) reported proteacean pollen, indicative of subhumid to semiarid lowland. The Proteaceae is one of the most diverse families in the Southern Hemisphere that is restricted to tropical and subtropical regions, especially in areas with long dry seasons (González et. al., 2007).

Sphagnum species dominate many wetlands and produce huge deposits of peat.

The statistical analysis of Paleocene–late Miocene palynological data from Patagonia supports several major stages of vegetation (Quattrocchio et al., 2013). The affinities of the fossil genera with the living ones (Romero, 1986) are based on physiognomic analyses of taphofloras, mainly from Chile and Argentina, warm and humid tropical conditions are inferred for the Paleocene-Eocene (Hinojosa, 2005). High rainfall and estimated temperatures for the Ligorio Márquez, Lota-Coronel and Cocholgüe taphofloras of the Paleocene-Eocene boundary are concordant with the tropical-subtropical climatic conditions inferred from its floristic composition. This analysis is based on the current correlation established between morphological characters of the leaves and climatic variables, basically, temperatures and rainfall (Hinojosa, 2005).

297 Paleoenvironmental reconstructions based on the Patagonian Paleocene floras of the
298 Salamanca and Bororó fomations enabled us to infer the presence of mangroves (with
299 *Nypa* palms and *Pandanus*), swamp woodlands, mossy forests and sclerophyllous forests
300 (Archangelsky, 1973; Petriella and Archangelsky, 1975).
301 The Paleocene flora is called the Gondwanic Paleoflora (Hinojosa, 2005) or Neotropical
302 (Romero, 1986). The Gondwanic Paleoflora was characterized by dominant Australasian,
303 Neotropical and Pantropical phytogeographical elements. The climate was warm and very
304 humid (mean annual temperature of 12.3–13°C, i.e., 1.5–2.5°C warmer than today, and
305 annual precipitation over 1000 mm, Iglesias et al., 2007).
306 In the early Eocene, the Subtropical Gondwanic Paleoflora of Hinojosa (2005) is
307 characterized by the mixture of Neotropical, Pantropical and Australasian taxa with a low
308 proportion of Antarctic elements.
309 The early Eocene was a globally warm period (Huber and Caballero, 2011; Lunt et al.,
310 2011). In Patagonia, the leaf floras yield estimated MATs of around 14–18 °C (Wilf et
311 al., 2005; Hinojosa et al., 2011) and mean annual precipitation of > 2000 mm (Wilf et al.
312 2009). No significant ice accumulation existed at high latitudes in either hemisphere
313 (Compagnucci, 2011).
314 The climate throughout Patagonia was humid and subtropical in the early Eocene; as the
315 humid easterlies (Atlantic monsoon) extended so far south that they dominated
316 continental Patagonia (Campagnucci, 2011).
317 The section analyzed (late Paleocene-Eocene) could be related to the Subtropical
318 Gondwanic Paleoflora of Hinojosa (2005) due to the presence of Antarctic (e.g.,
319 *Nothofagidites*), Australasian (e.g., *Dacrycarpidites*) and Pantropical (*Pandanus*)
320 elements. The spores of bryophytes and ferns are reported from the Antarctic Realm in

321 the Paleogene and are associated with pollen of *Nothofagus* (Morh et al., 2001 and
322 bibliography cited therein).
323 According to Carvajal (2013) the palynoflora of the Ligorio Márquez Formation
324 (Cordillera Patagónica Central of Chile, S 46° 45´, W 71° 50´) is a transition between a
325 Subtropical Godwanic and a Mixed Palynoflora. The unit is no older than 52 Ma (time of
326 the early Eocene Climate Optimum) and no younger than 47.6 Ma (Carvajal, 2013).
327 However, Suárez et al. (2000) concluded that the age was late Paleocene to early Eocene
328 based on newly collected plant megafossils, as well as on K-Ar ages for the overlying
329 basalt flows (Yabe, 2006).
330 The inferences of the Ligorio Márquez paleoclimate were made from Niche Modelling
331 Analysis of current relatives and Coexistence Analysis of taxa identified in the microflora.
332 The DCA (Detrended Correspondence Analysis) suggests similarity with the Punta Prat
333 locality (Chorrillo Chico and Agua Fresca formations). These unique formations share
334 the presence of *Nothofagidites kaitangataensis*, which is grouped as 'Ancestral'
335 *Nothofagidites* (Dettmann et al. 1990) that is exclusively fossil (Carvajal, 2013). This
336 taxon is also recorded in the La Barca Formation (in this paper).
337 Comparison of the present palynoflora with the late Paleocene-early Eocene Ligorio
338 Marquez Formation from Patagonia, Argentina (Macphail et al., 2013) yielded a fairly
339 similar palynological association (e.g., *Podocarpidites marwickii*, *Nothofagidites* spp.,
340 Proteaceae), but the La Barca Formation mainly lacks: *Ericipites microverrucatus*
341 (Ericales), *Mutisiapollis* sp. (Asteraceae), *Proxapertites* sp. (Araceae) and *Schizocolpus*
342 sp. (Didymelaceae).
343 The new record of Lactoridaceae expands the known fossil range of this family in
344 Patagonia. It was found in in Cerro Malvinera (*Rosannia manika* (Srivastava) Srivastava
345 and Braman, 2010), correlated with the La Barca Formation at the type locality of this

346 formation (Quattrocchio, 2017) (Fig. 1.A). Gamerro and Barreda (2008) found fossil
347 tetrads of Lactoridaceae and informally named them as 'Lactoris type' in the early
348 Miocene of eastern Patagonia.
349 From the comparison of the present microfloristic association with the Punta Prat locality
350 (Chorrillo Chico and Agua Fresca formations) the absence of the Lactoridaceae stands
351 out in the latter, but almost all the rest of the families are the same. In the late Paleocene-
352 early Eocene characterized by *Apectodinium* it is also not recorded. The absence of this
353 family could be related to the hiatus in that interval.
354 In the Magallanes-Austral Basin *Apectodinium* (as *Apectodinium* spp.) was first observed
355 in the Punta Noguera Formation (Olivero et al., 2002), assigned to the upper Paleocene
356 and Paleocene-Eocene on the basis of foraminifera and dinoflagellate cysts. In the
357 Tranquilo-2 well, Core T6 (1,205.04-1,205.10 m), near the Chile-Argentina border, 148
358 km from Punta Arenas, Morgan et al. (2000) briefly described the dinoflagellate cyst
359 assemblages including *Apectodinium homomorphum*. To the north, diverse marine
360 dinoflagellate cyst assemblages, including *Apectodinium homomorphum*, have been
361 recorded (Bijl et al., 2021) in outcrops at Isla Riesco in the Chorillo Chico Formation (S
362 52°40´24.71″, W 71°57´9.62″) and Agua Fresca Formation (S 52° 40´35.98″, W
363 71°56´57.27″) and also in the Laguna Blanca Río Pérez region in the Chorrillo Chico
364 Formation (S 52°32´1.56″, W 72° 6´22.41″). This taxon was also recorded in the Punta
365 Torcida Formation at its type locality (Quattrocchio, 2017).
366 *4.2. Paleoenviromental inferences based on palynological analysis*
367 Dinoflagellate cysts have been widely and successfully employed as paleoenvironmental
368 indicators (e.g., Downie et al., 1971; Wall et al., 1977; Dale, 1996; Pross and Brinkhuis,
369 2005; Frieling and Sluijs, 2018; Quattrocchio et al., 2021). The richness and abundance
370 of the dinoflagellate cyst assemblages recovered from the Chorrillo Chico and Agua

Fresca formations, Punta Prat locality, and from the La Barca Formation, Punta Ainol locality, allow us to evaluate the depositional environment of the studied sections during the Paleocene (Chorrillo Chico), early–late Eocene (Agua Fresca formations) and the Thanetian–Lutenian (La Barca Formation) intervals. The distribution diagrams of the dinoflagellate cyst species are shown in Tables 2 and 3. The ecogroup to which each taxon belongs and the paleoecological preferences of the ecogroups or taxa are given in Table 4.

4.2.1. Punta Prat Section. Chorrillo Chico and Agua Fresca formations

Two curves were plotted based on the spore abundance and paleoecological preferences of dinoflagellate cysts (ecogroups and taxa), one showing changes in the depositional environment of the Chorrillo Chico and Agua Fresca formations and the other portraying the terrigenous input to the basin (Fig. 2). The high sea level is interpreted based on the presence of outer neritic conditions or even oceanic taxa.

In the Chorrillo Chico Formation, the curves do not show any major oscillations except for the peaks in PP6 and PP12. The PP5–PP11 interval (no younger than late Selandian–Thanetian), would have been deposited mainly in an outer neritic environment with high-moderate terrigenous input, except for PP6, which may have accumulated in an oceanic environment with high terrigenous input. PP12 (Thanetian) would have been deposited in an oceanic environment with low terrigenous input.

In these same levels Carrillo-Berumen et al. (2013) identified a rich and abundant sporomorph association, especially in spores, a high abundance and richness of dinoflagellate cysts and the presence of *Impagidinium*, from which they suggested that the Chorrillo Chico Formation would have been deposited from hyperpycnal flows. The capacity of these flows to transport large volumes of sediment and organic matter from proximal to deep marine settings (Quattrocchio et al., 2018) would explain the co-

396 occurrence of dinoflagellate cysts indicative of low salinity and high nutrients related to
397 an increase in fresh-water runoff (e.g. *Senegalinium* complex, PAGC, *Paleocystodinium*
398 and *Paleoperidinium pyrophorum*) and dinoflagellate cysts indicative of outer neritic or
399 oceanic settings (e.g. *Spiniferites*, *Pyxidinopsis* and *Impagidinium*) (Fig. 2).
400 As previously mentioned, the deposition of sample PP12 would have accumulated in an
401 oceanic environment with low terrigenous input to the basin. This possibility, suggested
402 by the presence of *Impagidinium* and the low spore abundance, reinforces the idea that a
403 relative rise in sea level was present at the top of the outcrop of the Chorrillo Chico
404 Formation (Carrillo-Berumen et al., 2013).
405 In the Agua Fresca Formation the curves oscillate considerably, reflecting deposition in
406 oceanic (PP13-PP14, PP16, PP18, PP26 and PP27), outer neritic (PP15, PP17, PP21,
407 PP24, PP25) and inner neritic (PP19, PP20, PP22, PP23) settings with low to moderate
408 terrigenous input. From the evolutionary perspective, from the base to the top, the PP13–
409 PP18 interval (early Eocene) may have been deposited in an oceanic and outer neritic
410 setting with low terrigenous input. In PP19–PP20 interval (middle Eocene), a relative sea
411 level fall would have occurred and deposition would have taken place in an inner neritic
412 setting with increased terrigenous input (low to moderate). In the PP21–PP25 interval
413 (middle Eocene–late Eocene) the depositional environment would have deepened to
414 inner-outer neritic, the terrigenous input decreased and then gradually increased (low
415 terrigenous input). Finally, in the PP26–PP27 interval (late Eocene) a new deepening
416 would have occurred and deposition would have taken place in outer neritic and oceanic
417 settings with increased terrigenous input to the basin (low-moderate terrigenous input).
418 The changes in the depositional setting and in the terrigenous input to the basin
419 recognized fit quite well with what is expected from the sequence stratigraphy postulated
420 for the Agua Fresca Formation (Quattrocchio, 2009). It also correlates with the marine

421 palynomorph and paludal palynomorph index curves (Carrillo-Berumen et al., 2013),
422 reflecting relative sea level rise, e.g., from PP13–PP18 (presence of *Impagidinium*,
423 *Spiniferites*, high marine palynomorph index and low paludal palynomorph index), or the
424 expansion of nearshore environments, e.g., from PP19–PP20 (presence of
425 *Palaeocystodinium*, *Senegalinium* complex, Protoperidinioids, high paludal palynomorph
426 index and low marine palynomorph index). These relative sea level fluctuations could
427 have acted in conjunction with higher subsidence rates of the Magallanes-Austral Basin
428 with respect to sedimentation rates and sediment supply during most of the Thanetian–
429 Ypresian and Bartonian–Priabonian intervals (Bijl. et al., 2021). However, further
430 thermocronology data would help to improve the knowledge of such an important
431 climatical and biological Paleocene-Eocene transition (Dr. C. Jaramillo, pers. comm.).

432 *4.2.2. Punta Ainol Section. La Barca Formation*

433 From the base to the top, there are three clearly recognizable intervals, 0–44 m, 49–74 m
434 and 82–120 m (Fig. 3). The 0 to 44 m interval (Thanetian) would have accumulated in an
435 inner neritic environment with a moderate to high terrigenous input. The 49–74 m interval
436 (Thanetian–Ypresian) may have accumulated in oceanic and outer neritic environments
437 with a high terrigenous input. The 82 to 113 m interval (Ypresian–Lutenian) would have
438 been deposited in an inner-outer neritic environment with a moderate terrigenous input.
439 At 120 m (Lutenian) there would have been a relative fall in the sea level with only
440 records of sporomorphs.

441 The analysis of the curves suggests, from the base to the top, that from 0–74 m
442 (Thanetian–Ypresian) the depositional environment may have deepened from inner
443 neritic to mainly oceanic and the terrigenous input increased (moderate to high). In the
444 82–113 m interval (Ypresian–Lutenian) there would have been a relative fall in the sea

level to inner-outer neritic environments and a decrease in the terrigenous input (high to moderate). Finally, at 120 m expansion of the coastal environment may have occurred.

The co-occurrence of several species of the *Senegalinium* complex, Protoperidinioids, PAGC (indicative of low salinity and high nutrients) and *Impagidinium* (oceanic settings) would indicate a high terrigenous input to the deep basinal environment. The transport of terrigenous material to environments so far from the coast would require flows with high transport capacity. Thus, it is plausible that the transport and accumulation process responsible for the studied deposits of the La Barca Formation were hyperpycnal flows. This inference is supported by the recurrent (vertical and lateral) alternation of sedimentary structures without rheological boundaries and the abundant carbonized plant fragments present in these levels of the La Barca Formation, both features considered diagnostic criteria for the recognition of hyperpycnites (Ponce and Carmona, 2011a; Quattrocchio et al., 2018; Torres Carbonell and Olivero, 2019).

The possibility that the studied levels of the La Barca Formation had accumulated from hyperpycnal flows has previously been suggested in sedimentological, micropaleontological and palynological studies (Ronchi et al., 2015; Torres Carbonell and Olivero, 2019; Quattrocchio, 2020).

4.2.3. Paleoenvironmental synthesis

During the Thanetian, most of the Chorrillo Chico Formation (up to PP11) and the La Barca Formation would have accumulated from hyperpycnal flows. Furthermore, in the upper part of the Chorrillo Chico Formation (PP12) a relative sea level rise event that occurred during the Thanetian would be recognized. The depositional environment of the La Barca Formation continued to be dominated by hyperpycnal flows until the Lutenian. The changes in the depositional setting and in the terrigenous input to the Magallanes Basin identified at the top of the Chorrillo Chico Formation and in the Agua Fresca

Formation could probably be related to the interaction of relative sea level fluctuations and higher rates of basin subsidence with respect to sedimentation rates and sediment supply.

In both sections during the Thanetian interval (59.2 Ma–56 Ma) and Ypresian interval (56 Ma–48.1 Ma) the sedimentation rates are similar according to the ages assigned with biostratigraphy: ~20 m/Ma and ~6 m/Ma respectively (Dr. A. Folguera, pers. comm.). This suggests that in both areas the sedimentation rate would have been controlled mainly by relative sea level changes.

4.3. Geochemical inferences

4.3.1. Punta Prat section. Chorrillo Chico and Agua Fresca formations

In order to carry out a geochemical characterization of the sedimentary rocks from the Chorrillo Chico and Agua Fresca formations, the Punta Prat sequence was divided into three chemozones illustrated in Figure 2. The first interval, CZ-1P, covers almost the entire section of the Chorrillo Chico Formation, from PP1 to PP8 (Paleocene?), the second interval, CZ-2P, extends across the transition of the Chorrillo Chico-Agua Fresca formations, from PP9 to PP18 (late Paleocene-early Eocene), and the third interval (CZ-3P) includes the rest of the Agua Fresca Formation, from PP19 to PP27 (middle to late Eocene).

The first chemozone of the Punta Prat section (CZ-1P) presents a drop in TOC, HI, and P values, from the base to the middle of the interval, with similar behavior of the Rb/Sr ratio that could be related to the availability of bioelements and the fluctuations of organic matter accumulation with a contribution of a mixture of terrigenous and basin material. TIC and Ca, together with the Mn/Fe and Ti/Ca ratios, show a relative increase in their values throughout CZ-1P (Fig. 2), suggesting enhanced accumulation and preservation of $CaCO_3$, favored by oxic and alkaline conditions (Burn and Palmer, 2014). These relative

geochemical fluctuations could be related to relative sea level falls and the manifestation of critical condition for preservation of organic matter.

In the second study interval (CZ-2P), specifically at 124 m during the Thatenian-Ypresian transition, TOC, HI and P together with the Rb/Sr and Ti/Ca ratios show the highest CZ-2P values, suggesting a rapid relative sea level rise associated with increased subduction rates (Bijl et al. 2021), with a large input of material concentrated in bioelements (like phosphorous), derived from the intensely weathered Patagonian-Fuegian magmatic arc (Barbeau et al., 2009), which migrated seaward (recorded by the increase of the Rb/Sr and Ti/Ca ratios in Figure 2). Gavrilov et al. (1997) postulated that this event was associated with activation of organic-walled phytoplankton productivity that served as the main supply for the accumulation of marine organic matter (exhibited by rising values of HI and TOC). In contrast, TIC, Ca, and Mn/Fe show the lowest values of the interval (CZ-2P), proposing the development of anoxic conditions in deep marine successions, responsible for the lack or suppressed state of calcareous plankton communities due to the elevation of the calcite compensation depth (Jenkyns, 2010).

At the top of CZ-2P (late Ypresian), all geochemical parameters recovered the initial values of the interval, characterized by a decrease in TOC, HI, P, Rb/Sr and Ti/Ca, and an increase in TIC, Ca and Mn/Fe values, indicating a stage of relative sea level lowering and eustatic level recovery.

At the base of the last interval (CZ-3P), during the timing of a deep foreland basin from the late Ypresian to Bartonian (Bijl et al., 2021), TOC and HI concentration increase, but TIC, Ca and Mn/Fe behave inversely and decay, compared to the upper part of the lower interval (CZ-2P). These relative geochemical changes are associated with a new relative sea level rise event and could be associated with a switch in sediment provenance, characterized by accumulation of organic matter with notable presence of organic-walled

plankton and a low contribution of calcareous plankton communities (Barbeau et al., 2009).

At the top of CZ-3P (Priabonian), the values of the geochemical parameters fluctuate considerably, controlled by the relative sea level changes. TOC concentration shows the lowest value at the top, and the HI is similar in the two evaluated samples of the interval, due to changes in the conditions of accumulation and preservation of organic matter. In contrast, TIC, Ca and Mn/Fe have the highest values at the end of CZ-3P, reflecting higher carbonate contents, which could be associated with higher abundance of nannofossils. Meanwhile, the Rb/Sr and Ti/Ca ratios together with P show no relative changes throughout the CZ-3P (Fig. 2), reflecting an equilibrium in the fluctuations of terrigenous and marine organic matter accumulation.

4.3.2. Punta Ainol section. La Barca Formation

In order to characterize the geochemical trends of the Punta Ainol sequence (Fig. 3), the section was divided into three chemozones (CZ-A) based on the intervals defined by the palynomorph records, spore abundances and paleoecological dinoflagellate cysts preferences: CZ-1A (5 samples: 4440 to 4445) covers the 0-44 m interval (Thanetian), CZ-2A (6 samples: 4437 to 4439 and 4448 to 4449) includes 44 m to 74 m (Thanetian-Ypresian) and CZ-3A (7 samples: 4446 to 4447 and 4450 to 4454) which extends from 74 m to 120 m (Ypresian-Lutetian).

The TOC values exhibit a slight fluctuation between 1.11% and 1.33% throughout CZ-1A (Thanetian), but HI decays at the top of this zone in coincidence with the highest peak of Mn/Fe, proposing more alkaline and oxic conditions (Burn and Palmer, 2014) which favored the presence of $CaCO_3$, represented by the highest values of TIC and Ca reached in the top sample (4440) of CZ-1A. The drop of HI in the middle of CZ-1A (between 19-32m) might be influenced by the increase in Rb/Sr and Ti/Ca, indicating more weathering

and clastic input, characterized by a higher contribution of terrestrial and/or marine/lacustrine residual organic matter to the basin (Exon et al., 2001).

HI and TOC reached the minimum values at the beginning and the end of CZ-2A, in coincidence with the fluctuations of the Rb/Sr and Ti/Ca ratios, suggesting variations in the organic matter flux and changes in its composition with a higher proportion of terrestrial compounds, suggested by the low HI values. Conversely, TIC, Ca and the Mn/Fe ratio reached the highest values of the entire sequence indicating oxic conditions that increase biogenic skeletal material from calcareous nannoplankton and foraminifera (Sageman and Lyons, 2004). These stages could be related to relative sea level falls that favor pelagic biogenic carbonate contribution versus organic phytoplankton productivity, associated with critical condition for organic matter accumulation.

In the middle of CZ-2A (Thanetian-Ypresian boundary), coincident with 62m, TOC, HI and P with the Rb/Sr and Ti/Ca ratios suddenly rise up and reach the highest values of this zone. This episode could be interpreted as a rapid transgression (Malumián, 1999) associated with the eustatic sea level rise (Haq et al., 1987). This event caused insoluble and dissolved organic matter, bioelements such as P, Fe, and other compounds accumulated in humid terrestrial areas during the preceding relative low sea level stage to bewere supplied to the basin. The enhancement of nutrients generated a vigorous phytoplankton productivity that served as the main provider of organic matter (Gavrilov et al., 1997) characterized by elevated values of HI (Shcherbinina et al., 2016). In contrast, TIC, Ca, and Mn/Fe dropped sharply until they reached the lowest values of the entire sequence. Gavrilov and Shcherbinina (2003) suggested that these changes could be accompanied by dramatic turnover from predominantly calcareous plankton communities to organic-walled plankton forming enormous biomasses and initiating accumulation of TOC and HI rich sediments.

570 This middle level of CZ-2A of the La Barca Formation accumulation was evidently
571 caused by a greatly enhanced supply of nutrients, which stimulated a burst of productivity
572 in the basin. Such increased fertilization could be induced by hyperpycnal flows, during
573 the relative sea level rise.

574 At the base of CZ-3A (early Ypresian), TOC, HI, TIC and Ca show very low values,
575 suggesting a decrease in the community of calcareous plankton and organic walls, such
576 as dinoflagellate cysts and nannofossils, related to relative sea level lowering and shoaling
577 of the basin (Shcherbinina et al., 2016). TOC and HI values increase towards the top of
578 CZ-3A (Ypresian-Lutenian), accompanied by a slight increase in Rb/Sr, Ti/Ca and P, a
579 drop in the Mn/Fe ratios and constant TIC and Ca values. However, there is a notorious
580 drop in the HI values at the top level of the Punta Ainol section (120 m), suggesting an
581 increase of terrigenous organic matter proportion (only sporomorphs are recorded),
582 characterized by lower TOC values. The behavior of the geochemical parameters along
583 the CZ-3A suggests a variation in the source of organic matter, characterized by
584 fluctuations from terrigenous to marine organic matter accumulation, and then, an
585 increase in the proportion of terrigenous organic matter towards the top, reflecting relative
586 sea level rise in the middle (82 m to 108 m) and the consequent sea level fall at the end.

587 *4.3.3. Geochemical synthesis*

588 The geochemical parameters from the La Barca Formation at Punta Ainol and a few
589 samples from the top of the Chorrillo Chico Formation from the Punta Prat section show
590 a vast increase in sediment supply from the continent with high concentrations of
591 nutrients, which stimulated a burst of productivity in the basin during Paleocene-Eocene
592 transition. These processes could be interpreted as hyperpycnal flows, characterized by
593 an increase in terrestrial weathering and the consequent supply of extrabasinal materials
594 (typically plant debris), fresh water and chemicals to environments far from the coast.

595 The CIE that characterized the Paleocene-Eocene Thermal Maximum (PETM) was not
596 identified in the Punta Prat section. The carbon isotope density values obtained were in
597 the order of -10‰ or -15‰, suggesting that the vast majority of the carbonate did not
598 derive from plankton but was precipitated in sediment pore waters with a low density of
599 ^{13}C due to organic matter remineralization. So, carbon isotope values from Punta Prat
600 would not be reliable for consideration in this study (Prof. Dr. A. Sluijs, 2022, pers.
601 comm., Paleoceanography, Earth Sciences Department of Utrecht, Utrecht, Netherlands).
602 Despite the lack of the CIE record that characterized the PETM, the Punta Ainol section
603 provides geochemical data related to characteristic processes of the Paleocene-Eocene
604 transition, recorded in other type localities around the world, such as significant increases
605 in river discharge and sediment input (e.g. Crouch et al., 2003; Giusberti et al., 2007; John
606 et al., 2008; Sluijs et al., 2008), sudden increases in organic microfossil productivity and
607 decreases in the amount of biogenic calcite (Sluijs et al., 2011), changes in trophic level
608 (e.g. Crouch et al., 2001; Speijer and Wagner, 2002; Gibbs et al., 2006), as well as a
609 globally recorded rise in sea level (Gavrilov et al., 1997), suggesting a link between
610 phases of extreme global warming phases and sea level change (Sluijs et al., 2008).
611

612 **5. Conclusions**

613 In this paper the comparison between the thick Paleogene sequences in the Chilean
614 Peninsula Brunswick (Chorrillo Chico and Agua Fresca formations) and the reduced
615 Paleogene sequence (La Barca Formation) in Argentina are evaluated by taking account
616 of palynological and geochemical analyses.
617 Warm and humid subtropical conditions (Subtropical Gondwanic Paleoflora) are inferred
618 for the late Paleocene-Eocene interval studied. The new record of the Lactoridaceae in
619 the La Barca Formation expanded the known fossil range of this family in Patagonia.

The comparison of the Punta Prat locality (Chorrillo Chico and Agua Fresca formations) with the Ainol locality (La Barca Formation) shows the absence of Lactoridaceae in the former, but almost all the rest of the families are the same. The late Paleocene–early Eocene characterized by *Apectodinium* is not recorded either. Both absences could be related to a hiatus in that interval.

During the late Paleocene the Chorrillo Chico and La Barca formations would have been deposited mainly from hyperpycnal flows. The depositional environment of the La Barca Formation continued to be dominated by hyperpycnal flows until the Lutenian.

A relative sea level rise event would be recognized in both sections studied in the early Eocene. In the middle Eocene a relative sea level fall would have occurred with increased terrigenous influx. These fluctuations could have been acting together with higher subsidence rates of the Magallanes-Austral Basin during most of the Thanetian–Ypresian and Bartonian–Priabonian.

The rate of sedimentation according to the ages assigned by biostratigraphy were similar during the Thanetian and Ypresian intervals in both sections, suggesting that the sedimentation rate would have been controlled mainly by relative sea level changes during the Paleocene-Eocene transition.

The increase in the organic phytoplancton productivity and notable decrease in the amount of biogenic calcite, associated with an increased sediment supply in a high sea level stage, suggested by geochemical and paleoecological parameters in the Punta Ainol section, eastern Tierra del Fuego, provide an opportunity to further understand the paleoenvironmental change in high southern latitudes during the greenhouse world of the late Paleocene-early Eocene transition. This would be reinforced by the presence of *Apectodinium* (Quattrocchio, 2021) and nannofossils characteristic of this interval (Bedoya Bedoya Agudelo et al., 2018).

Acknowledgements

Special thanks to Dr. Eduardo Olivero for the outcrops samples of the La Barca Formation. The author would like to thank the handling editor Dr. Francisco J. Vega, and reviewers Dr. Carlos Jaramillo, Dr. Andrés Folguera and anonymous reviewer for their careful reading of our manuscript and their many insightful comments and suggestions, which significantly improved this paper. The Authors also thank to Gastón Otegui and Raúl Guanco from the Geochemical Laboratory of Y-TEC (YPF Tecnología) for geochemistry analysis. This work was supported by the Secretary of Science and Technology at the National University of the South (SEGCyT) under Grant [PGI-24/ H156.-M.A. Martínez].

References

Arai, M., Viviers, M.C., 2013. Dinoflagellate cyst superdominance assemblages from the Upper Cretaceous of the Santos Basin, offshore SE Brazil, and their palaeoecological significance, in: Lewis, J.M., Marret, F., Bradley, L.R. (Eds.), Biological and Geological Perspectives of Dinoflagellates. Geological Society of London, pp. 285–292. https://doi.org/10.1144/TMS5.27

Archangelsky, S., 1973. Palinología del Paleoceno de Chubut. I. Descripciones Sistemáticas. Ameghiniana 10, 339-399.

Askin, R.A., 1988. The palynological record across the Cretaceous/Tertiary transition on Seymour Island, Antarctica, in: Feldmann, R.M., Woodburne, M.O. (Eds.), Geology and Paleontology of Seymour Island Antarctic Peninsula. Geological Society of America 169, 155–162. https://doi.org/10.1130/MEM169-p155

669 Barbeau, D.L., Olivero, E.B., Swanson-Hysell, N.L., Zahid, K.M., Murray, K.E., Gehrels,
670 G.E., 2009. Detrital-zircon geochronology of the eastern Magallanes foreland basin:
671 Implications for Eocene kinematics of the northern Scotia Arc and Drake Passage. Earth
672 and Planetary Science Letters 284 (3-4), 489-503. https://doi:
673 10.1016/j.epsl.2009.05.014.

674 Barreda, V.D., 1996. Bioestratigrafía de polen y esporas de la Formación Chenque,
675 Oligoceno tardío-Mioceno de las provincias de Chubut y Santa Cruz, Patagonia,
676 Argentina. Ameghiniana 33, 35–96.

677 Bedoya, Agudelo E.L., Olivero, E.B., Concheyro, A., Torres Carbonell, P.J., Martinioni,
678 D.R., 2018. Calcareous nannofossils from the La Barca Formation (Paleocene/Eocene
679 boundary), Tierra del Fuego, Argentina. Ameghiniana 55 (2), 223–229.

680 Behar, F., Beaumont, Y., De, B., Penteado, H.I., 2001. Rock-eval 6 technology:
681 performances and developments. Oil & Gas Science and Technology – Revue Institut
682 Francais Du Petrole 56 (2), 111-134.

683 Biddle, K.T., Uliana, M.A., Mitchum Jr, R.M., Fitzgerald, M.G., Wright, R.C., 1986. The
684 Stratigraphic and Structural Evolution of the Central and Eastern Magallanes Basin,
685 Southern South America, in: Foreland Basins. John Wiley & Sons, Ltd, pp. 41–61.
686 https://doi.org/10.1002/9781444303810.ch2

687 Bijl, P.K., Sluijs, A., Brinkhuis, H., 2013. A magneto- and chemostratigraphically
688 calibrated dinoflagellate cyst zonation of the early Palaeogene South Pacific Ocean.
689 Earth-Science Reviews 124, 1–31.

690 Bijl, P.K., Guerstein, G.R., Sanmiguel Jaimes, E.A., Sluijs, A., Casadio, S., Valencia, V.,
691 Amenábar, C.R., Encinas, A., 2021. Campanian-Eocene dinoflagellate cyst

692 biostratigraphy in the Southern Andean foreland basin: Implications for Drake Passage
693 throughflow. Andean Geology 48 (2): 185-218. https://doi: 10.5027/andgeoV48n2-3339

694 Bujak, J., Brinkhuis, H., 1998. Global warming and dinocyst changes across the
695 Paleocene/Eocene Epoch boundary. In: Aubry M.P., et al., (Eds.), Late Paleocene-Early
696 Eocene biotic and climatic events in the marine and terrestrial records. New York,
697 Columbia University Press, pp. 277–295.

698 Brinkhuis, H., 1994. Late Eocene to Early Oligocene dinoflagellate cysts from the
699 Priabonian type-area (Northeast Italy): biostratigraphy and paleoenvironmental
700 interpretation. Palaeogeography, Palaeoclimatology, Palaeoecology 107, 121–163.
701 https://doi.org/10.1016/0031-0182(94)90168-6

702 Brinkhuis, H., Powell, A.J., Zevenboom, D., Head, M.J., Wrenn, J.H., 1992. High-
703 resolution dinoflagellate cyst stratigraphy of the Oligocene/Miocene transition interval in
704 northwest and central Italy. Neogene and Quaternary Dinoflagellate Cysts and Acritarchs.
705 American Association of Stratigraphic Palynologists Foundation, Dallas 219, 258.

706 Brinkhuis, H., Zachariasse, W.J., 1988. Dinoflagellate cysts, sea level changes and
707 planktonic foraminifers across the Cretaceous-Tertiary boundary at El Haria, northwest
708 Tunisia. Marine Micropaleontology 13, 153–191. https://doi.org/10.1016/0377-
709 8398(88)90002-3

710 Buggle, B., Glaser, B., Hambach, U., Gerasimenko, N., Markovic, S., 2011. An
711 evaluation of geochemical weathering indices in loess-paleosol studies. Quaternary
712 International 240, 12-21.

713 Burn, M.J., Palmer, S.E., 2014. Solar forcing of Caribbean drought events during the last
714 millennium. Journal of Quaternary Science 29, 8, 827–836. https://doi:10.1002/jqs.2660

715 Candel, M.S., Díaz, P.E., Borromei, A.M., Fernández, M., Montes, A., Santiago, F.C.,
716 2020. Multiproxy analysis of a Lateglacial-Holocene sedimentary section in the Fuegian
717 steppe (northern Tierra del Fuego, Argentina): Implications for coastal landscape
718 evolution in relation to climatic variability and sea-level fluctuations. Palaeogeography,
719 Palaeoclimatology, Palaeoecology 557, 109941.

720 Carbajal, M.M., 2013. Paleoclima y diversidad en la palinoflora de la Formación Ligorio
721 Márquez. Ph.D. Thesis, Facultad de Ciencias, Universidad de Chile, Chile.

722 Carrillo-Berumen, R., Quattrocchio, M.E., Helenes, J., 2013. Palinomorfos continentales
723 del Paleógeno de las formaciones Chorrillo Chico y Agua Fresca, Punta Prat, Región de
724 Magallanes, Chile. Andean Geology 40 (3), 539-560.

725 Castro, S.P., Carvalho, M.A., 2015. Santonian dinocyst assemblages of the Santa Marta
726 Formation, Antarctic Peninsula: Inferences for paleoenvironments and paleoecology. An.
727 Acad. Bras. Ciênc. 87, 1583–1597. https://doi.org/10.1590/0001-3765201520140651

728 Chen, J., An, Z.S., Head, J., 1999. Variation of Rb/Sr Ratios in the Loess-Paleosol
729 Sequences of Central China during the Last 130 000 Years and Their Implications for
730 Monsoon. Paleoclimatology. Quaternary Research 51, 215–219.

731 Compagnucci, R.H., 2011. Atmospheric circulation over Patagonia from the Jurassic to
732 present: a review through proxy data and climatic modelling scenarios. Biological Journal
733 of the Linnean Society 103, 229–249.

734 Crouch, E.M., 2001. Environmental change at the time of the Paleocene-Eocene Biotic
735 Turnover. LPP contributions series, Vol. 14. Utrech, 216 p.

736 Crouch, E.M., Heilmann-Clausen, C., Brinkhuis, H., Morgans,H.E.G. Rogers, K.M.,
737 Egger, H., Schmitz, B., 2001. Global dinoflagellate event associated with the late
738 Paleocene thermal maximum, Geology 29, 315-318.

739 Crouch, E.M., Dickens G.R., Brinkhuis H., Aubry M-P., Hollis C.J., Rogers K.M.,
740 Visscher H., 2003. The Apectodinium acme and terrestrial discharge during the
741 Paleocene–Eocene thermal maximum: new palynological, geochemical and calcareous
742 nannoplankton observations at Tawanui, New Zealand. Palaeogeography,
743 Palaeoclimatology, Palaeoecology 194 (4), 387–403.

744 Crouch, E.M., Brinkhuis, H., 2005. Environmental change across the Paleocene-Eocene
745 transition from eastern New Zealand: A marine palynological approach. Marine
746 Micropaleontology 56, 138-160.

747 Crouch, E.M., Willumsen, P.S., Kulhanek, D.K., Gibbs, S., 2014. A revised Paleocene
748 (Teurian) dinoflagellate cyst zonation from eastern New Zealand. Review of
749 Palaeobotany and Palynology 202, 47–79.

750 Cuciniello, C.D., Perez Panera, J.P., Bedoya Agudelo, E.L., Olivero, E., 2017.
751 Morfogrupos de foraminíferos bentónicos aglutinados del Miembro LB2, Formación La
752 Barca, en el área de Cabo José-Punta Ainol (Paleoceno, Cuenca Austral, Argentina). XX
753 Congreso Geológico Argentino; San Miguel de Tucumán, Argentina, 12–14.

754 Cybulska, D., Rubinkiewicz, J., 2020. The Apectodinium spp. acme as an evidence for
755 the Paleocene-Eocene termal maximum from the Polish Outer Carpathians. Geological
756 Quarterly 64 (2), 241–251. http://dx.doi.org/10.7306/gq.1521.

757 Dale, B., 1996. Dinoflagellate cyst ecology: modeling and geological applications.
758 Palynology: principles and applications 3, 1249–1275.

759 Dasch, E. J., 1969. Strontium isotopes in weathering profiles, deep-sea sediments, and
760 sedimentary rocks. Geochimica et Cosmochimica Acta 33, 1521–1552.
761 https://doi.org/10.1016/0016-7037(69)90153-7

762 Davison, W., 1993. Iron and manganese in lakes. Earth Science Reviews 34, 119–163.

763 Deaf, A.S., Harding, I.C., Marshall, J.E.A., 2020. Cretaceous (Hauterivian–Cenomanian)
764 palaeoceanographic conditions in southeastern Tethys (Matruh Basin, Egypt):
765 Implications for the Cretaceous climate of northeastern Gondwana. Cretaceous Research
766 106, 104229. https://doi.org/10.1016/j.cretres.2019.104229

767 Decat, J., Pomeyrol, R. 1931 Informe geológico sobre las posibilidades petrolíferas de la
768 Región Magallánica. Boletín Minero, Sociedad Nacional de Minería 389 (43), 763–772.

769 Dettmann, M., Pocknall, D., Romero, E., Zamaloa, M.C.,1990. Nothofagidites Erdtman
770 ex Potonie, 1960; a catalogue of species with notes on the paleogeographic distribution
771 of Nothofagus B1. (Southern Beech). New Zealand Geological Survey Paleontological
772 Bulletin 60, 1-79.

773 Downie, C., Hussain, M.A., Williams, G.L., 1971. Dinoflagellate cyst and acritarch
774 associations in the paleogene of Southeast England. Geoscience and Man 3, 29–35.
775 https://doi.org/10.1080/00721395.1971.9989706

776 ENAP, 1992. Field trip guidebook Brunswick Peninsula área, in: Cortés, R., Herrero, C.
777 (Eds.), Empresa Nacional del Petróleo Punta Arenas, pp. 1-27.

778 Eshet, Y., Almogi-Labin, A., Bein, A., 1994. Dinoflagellate cysts, paleoproductivity and
779 upwelling systems: A Late Cretaceous example from Israel. Marine Micropaleontology
780 23, 231–240. https://doi.org/10.1016/0377-8398(94)90014-0

781 Exon, N.F., Kennett, J.P., and Malone, M.J., 2001. Proceedings of the Ocean Drilling
782 Program, 189 Initial Reports: College Station, TX (Ocean Drilling Program), 1–37.
783 https://doi:10.2973/odp.proc.sr.189.101.2004

784 Frieling, J., Sluijs, A., 2018. Towards quantitative environmental reconstructions from
785 ancient non-analogue microfossil assemblages: Ecological preferences of Paleocene –
786 Eocene dinoflagellates. Earth-Science Reviews 185, 956–973.
787 https://doi.org/10.1016/j.earscirev.2018.08.014

788 García, V.M., Quattrocchio, M.E., Zavala, C.A., Martínez, M.A., 2006. Palinofacies,
789 paleoambientes y paleoclima del Grupo Cuyo (Jurásico Medio) en la Sierra de Chacaico,
790 Cuenca Neuquina. Revista Española de Micropaleontología 38 (2-3), 191-210.

791 Gavrilov, Y.O., Kodina, L.A., Lubchenko, I.Y., Muzylöv, N.G., 1997. The late Paleocene
792 anoxic event in epicontinental seas of Peri-Tethys and formation of sapropelite unit:
793 sedimentology and geochemistry. Lithology and Mineral Resources 35, 427-450.

794 Gavrilov, Y.O., Shcherbinina, E.A., 2003. Dynamics of propagation of the biospheric
795 event at the PaleoceneEocene Transition. Conference: Climate and Biota of the Early
796 Paleogene. Volume of Abstracts, Bilbao, Spain. 50.

797 Gibbs, S.J., Bralower, T.J., Bown, P.R., Zachos, J.C., Bybell, L M., 2006. Shelf and open-
798 ocean calcareous phytoplankton assemblages across the Paleocene-Eocene Thermal
799 Maximum: Implications for global productivity gradients. Geology 34, 233-236.

800 Giusberti, L., Rio, D., Agnini, C., Backman, J., Fornaciari, E., Tateo, F., and Oddone, M.,
801 2007. Mode and tempo of the Paleocene-Eocene thermal maximum in an expanded
802 section from the Venetian pre-Alps. Geological Society of America Bulletin 119, 391-
803 412.

804 Gradstein, F.M., Ogg, J.G., 2020. Chapter 2 - The Chronostratigraphic Scale, in:
805 Gradstein, Felix M., Ogg, James G., Schmitz, M.D., Ogg, G.M. (Eds.), Geologic Time
806 Scale 2020. Elsevier, pp. 21–32. https://doi.org/10.1016/B978-0-12-824360-2.00002-4

807 Greenwood, D.R., Moss, P.T., Rowett, A.I., Vadala, A.J., Keefe, R.L., 2003. Plant
808 communities and climate change in southeastern Australia during the early Paleogene, in:
809 Wing, S.L., Gingerich, P.D., Schmitz, B., Thomas, E. (Eds.), Causes and Consequences
810 of Globally Warm Climates in the Early Paleogene. Geological Society of America 369,
811 365–380. https://doi.org/10.1130/0-8137-2369-8.365

812 Guerstein, G.R., González Estebenet, M.S., Alperín, M.I., Casadío, S.A., Archangelsky,
813 S., 2014. Correlation and paleoenvironments of middle Paleogene marine beds based on
814 dinoflagellate cysts in southwestern Patagonia, Argentina. Journal of South American
815 Earth Sciences 52, 166–178. https://doi.org/10.1016/j.jsames.2014.02.011

816 Guerstein, G.R., Guler, M.V., Brinkhuis, H., Warnaar, J., 2010. Mid cenozoic
817 palaeoclimatic and palaeoceanographic trends in the southwest Atlantic basins, a
818 dinoflagellate view., in: Madden, R.H., Carlini, A.A., Vucetich, M.G., Kay, R.F. (Eds.),
819 The Paleontology of Gran Barranca: Evolution and Environmental Change through the
820 Middle Cenozoic of Patagonia. Cambridge, Cambridge University Press, Cambridge, pp.
821 398–409.

822 Guler, M.V., Borel, C.M., Brinkhuis, H., Navarro, E.L, Astini, R.A, 2014. Brackish to
823 Freshwater Dinoflagellate Cyst Assemblages from the la Colonia Formation
824 (Paleocene?), Northeastern Patagonia, Argentina. Ameghiniana 51, 141–153, 13.

825 Guler, M.V., González Estebenet, M.S., Navarro, E.L., Astini, R.A., Pérez Panera, J.P.,
826 Ottone, E.G., Pieroni, D., Paolillo, M.A., 2019. Maastrichtian to Danian Atlantic

827 transgression in the north of Patagonia: A dinoflagellate cyst approach. Journal of South
828 American Earth Sciences 92, 552–564. https://doi.org/10.1016/j.jsames.2019.04.002

829 Gustafsson, C., 2000. Three New South American Species of Randia (Rubiaceae,
830 Gardenieae) Novon A Journal for Botanical Nomenclature 10, 201-208
831 https://doi:10.2307/3393100

832 Harris, A.J., Tocher, B.A., 2003. Palaeoenvironmental analysis of Late Cretaceous
833 dinoflagellate cyst assemblages using high-resolution sample correlation from the
834 Western Interior Basin, USA. Marine Micropaleontology 48, 127–148.
835 https://doi.org/10.1016/S0377-8398(03)00002-1

836 Haq, B.U., Hardenbol, J., Vail, P.R., 1987. Chronology of fluctuating sea levels since the
837 Triassic. Science 235, 1156–1167. http://doi:10.1126/science.235.4793.1156

838 Hinojosa, L.F., 2005. Cambios climáticos y vegetacionales inferidos a partir de
839 paleofloras cenozoicas del sur de Sudamérica. Revista Geológica de Chile 32, 95–115.

840 Hinojosa, L.F., Villagran, C., 1997. Historia de los bosques del sur de Sudamérica. I:
841 antecedentes paleobotánicos, geológicos y climáticos del Terciario del cono sur de
842 America. Revista Chilena de Historia Natural 70, 225–239.

843 Hinojosa, L.F., Perez, F., Gaxiola, A., Sandoval, I., 2011. Historical and phylogenetic
844 constraints on the incidence of entire leaf margins: insights from a new South American
845 model. Global Ecology and Biogeography 20, 380–390.

846 Huber, M., Caballero, R., 2011. The early Eocene equable climate problem revisited.
847 Climate of the Past 7, 603–633.

848 Iglesias, A., Wilf, P., Johnson, K.R., Zamuner, A.B., Cuneo, N.R., Matheos, S.D., Singer,
849 B.S., 2007. A Paleocene lowland macroflora from Patagonia reveals significantly greater
850 richness than North American analogs. Geology 35, 947–950.

851 Ingram, W.C., Meyers, S.R., Martens, C.S., 2013. Chemostratigraphy of deep-sea
852 Quaternary sediments along the Northern Gulf of Mexico Slope: Quantifying the source
853 and burial of sediments and organic carbon at Mississippi Canyon 118. Marine and
854 Petroleum Geology 46, 190-200.

855 Jenkyns, H.C., 2010. Geochemistry of oceanic anoxic events. Geochemistry, Geophysics,
856 Geosystems 11 (3), 1-30. https://doi:10.1029/2009GC002788.

857 John, C.M., Bohaty, S.M., Zachos, J.C., Sluijs, A., Gibbs, S.J., Brinkhuis, H., Bralower,
858 T.J., 2008. North American continental margin records of the Paleocene-Eocene thermal
859 maximum: Implications for global carbon and hydrological cycling. Paleoceanography
860 23, PA2217. https://doi:2210.1029/2007PA001465, 2008.

861 Kennett, J.P., Stott, L.D., 1991. Abrupt deep-sea warming, palaeoceanographic changes
862 and benthic extinctions at the end of the Palaeocene. Nature 353, 225–229.

863 Koch, P.L., Zachos, J. C., Gingerich, P.D., 1992. Correlation between isotope records in
864 marine and continental carbon reservoirs near the Palaeocene/Eocene boundary. Nature
865 358, 319-322.

866 Koinig, K.A., Shotyk, W., Lotter, A.F., Ohlendorf, C., Sturm, M., 2003. 9000 years of
867 geochemical evolution of lithogenic major and trace elements in the sediment of an alpine
868 lake - the role of climate, vegetation and land-use history. Journal of Paleolimnology 30,
869 307–320.

870 Kujau, A., Nurnberg, D., Zielhofer, C., Bahr, A., Rohl, U., 2010. Mississippi River
871 discharge over the last 560,000 years. Indications from X-ray fluorescence core-scanning.
872 Palaeogeography, Palaeoclimatology, Palaeoecology 298, 311-318.

873 Lamolda, M.A., Mao, S., 1999. The Cenomanian–Turonian boundary event and dinocyst
874 record at Ganuza (northern Spain). Palaeogeography, Palaeoclimatology, Palaeoecology
875 150, 65–82. https://doi.org/10.1016/S0031-0182(99)00008-5

876 Litt, T., Krastel, S., Sturm, M., Kipfer, R., Örcen, S., Heumann, G., Sven, S.O., Ülgen,
877 U.B., Niessen, F., 2009. 'PALEOVAN', International Continental Scientific Drilling
878 Program (ICDP): site survey results and perspectives. Quaternary Science Reviews 28,
879 1555-1567.

880 Löwemark, L., Chen, H.F., Yang T.N., Kylander, M., Yu, E.F., Hsu, Y.W., Lee, T.Q.,
881 Song, S.R., Jarvis, S., 2011. Normalizing XRF scanner data: a cautionary note on the
882 interpretation of high-resolution records from organic-rich lakes. Journal of Asian Earth
883 Sciences 40, 1250–1256.

884 Lunt, D.J., Ridgwell, A., Sluijs, A, Zachos, J., Hunter, S., Haywood, A., 2011. A model
885 for orbital pacing of methane hydrate destabilization during the Palaeogene. Nature
886 Geosciences 4, 775–778.

887 Mackenzie, F.T., Ver, L.M., Sabine, C., Lane, M., Lerman, A., 1993. C, N, P, S global
888 biogeochemical cycles and modelling of global change. In: Wollast, R., Mackenzie, F.T.,
889 Chou, L. (Eds.), Interactions of C, N, P and S, Biogeochemical Cycles and Global
890 Changes. NATO ASI series. I 4, 1-61.

891 Macphail, M., Carpenter, R.J., Iglesias, A., Wilf, P., 2013. First Evidence for Wollemi
892 Pine-type Pollen (Dilwynites: Araucariaceae) in South America. PLoS ONE 8(7):
893 e69281. https://doi.org/10.1371/journal.pone.0069281

894 Malumián, N., 1999. La sedimentación en la Patagonia extraandina. In Geología
895 Argentina, R. Caminos Ed. Servicio Geológico Argentino, Anales 29, 557-578.

896 Malumián, N., Hromic, T., Nañez, C., 2013. The Paleogene of the Magallanes basin:
897 biostratigraphy and unconformities. Anales Instituto Patagonia (Chile) 41(1) 29–52.

898 Martinez-Pardo, R.,1971. Relaciones cronoestratigráficas a lo largo del Territorio
899 Chileno durante el Cenozoico. Geochile (Asociación Geológica de Chile), 35–43

900 Meyers, S.R., Sageman, B.B., 2004. Detection, quantification, and significance of
901 hiatuses in pelagic and hemipelagic strata. Earth and Planetary Science Letters 224, 55-
902 72.

903 Morgan, H.E.G., Wilson, G.J., Strong, C.P., Crundwell, M.P., 2000. Southern
904 Hemisphere Cretaceous–Cenozoic paleoceanographic and paleoclimatic events II:
905 foraminiferal and dinoflagellate biostratigraphy of southern Patagonian field collections
906 (March–April 2000), New Zealand: Institute of Geological and Nuclear Sciences 19, 15p.

907 Morh, B.A.R., 2001. The development of Antarctic fern floras during the Tertiary, and
908 palaeoclimatic and palaeobiogeographic implications. Palaeontographica Abteilung B
909 259, 167-208.

910 Natland, M.L., Eduardo, G.P., Cañon, A., Ernst, M., 1974. A System of Stages for
911 Correlation of Magallanes Basin Sediments, in: Natland, M.L., Gonzalez P., E., Canon,
912 A., Ernst, M. (Eds.), A System of Stages for Correlation of Magallanes Basin Sediments.
913 Geological Society of America, p. 0. https://doi.org/10.1130/MEM139-p1

914 Olivero. E.B., Malumian. N., Palamarczuk. S., Scasso. R.A., 2002. El Cretácico Superior-
915 Paleógeno del área del Río Bueno, costa atlántica de la Isla Grande de Tierra del Fuego.
916 Revista de la Asociación Geológica Argentina 57, 199–218.

Olivero. E.B., Malumián. N., 2008. Mesozoic-Cenozoic stratigraphy of the Fuegian Andes, Argentina. Geological Acta 6 (1), 5–18.

Pattan, J.N., Masuzawa, T., Borole, D.D., Parthiban, G., Jauhari, P., Yamamoto, M., 2005. Biological productivity, terrigenous influence and noncrustal elements supply to the Central Indian Ocean Basin: paleoceanography during the past » 1 Ma. Journal of Earth System Science 114,1, 63-74.

Peters, K.E., 1986. Guidelines for evaluating petroleum source rock using programmed pyrolysis. AAPG Bulletin 70, 318-86.

Petriella, B., Archangelsky, S., 1975. Vegetación y ambiente en el Paleoceno de Chubut. 1st. Congreso Argentino de Paleontología y Bioestratigrafía, Tucumán, Actas 2, 257–270.

Peyrot, D., 2011. Late Cretaceous (Late Cenomanian–Early Turonian) dinoflagellate cysts from the Castilian Platform, northern Spain. Palynology 35, 267–300. https://doi.org/10.1080/gspalynol.35.2.267

Ponce, J.J., Carmona, N., 2011a. Coarse-grained sediment waves in hyperpycnal clinoform systems, Miocene of the Austral foreland basin, Argentina. Geology 39, 763–766. https://doi.org/10.1130/G31939.1

Powell, A.J., Brinkhuis, H., Bujak, J.P., 1996. Upper Paleocene-Lower Eocene dinoflagellate cyst sequence biostratigraphy of southeast England. Geological Society, London, Special Publications 101, 145–183. https://doi.org/10.1144/GSL.SP.1996.101.01.10

938 Prauss, M.L., 2012. The Cenomanian/Turonian Boundary event (CTBE) at Tarfaya,
939 Morocco: Palaeoecological aspects as reflected by marine palynology. Cretaceous
940 Research 34, 233–256. https://doi.org/10.1016/j.cretres.2011.11.004

941 Prevot, L., Lucas, J., Doubinger, J., 1979. A note on the palynological contents, mineral
942 composition and chemistry of a sedimentary phosphate series (Ganntour, Maroc).
943 Sciences Geologiques Bulletin 32 (1), 69–90.

944 Pross, J., Brinkhuis, H., 2005. Organic-walled dinoflagellate cysts as paleoenvironmental
945 indicators in the Paleogene; a synopsis of concepts. Paläontol Z 79, 53–59.
946 https://doi.org/10.1007/BF03021753

947 Quattrocchio, M.E., 2009. Paleogene dinoflagellate cysts from Punta Prat, southern Chile.
948 Palynology 33 (1), 141–156.

949 Quattrocchio, M.E., 2017. New fossil record of Lactoridaceae in the Paleogene of
950 southern Patagonia (South America). Revista Del Museo Argentino de Ciencias Naturales
951 (n.s.) 19, 71–84.

952 Quattrocchio, M.E., 2021. Late Paleocene–middle Eocene dinoflagellate cysts from the
953 La Barca Formation, Austral Basin, Argentina, Palynology 45 (3), 421-428.

954 Quattrocchio, M.E., Sarjeant, W.A.S., 2003. Dinoflagellates from the Chorrillo Chico
955 Formation (Paleocene) of southern Chile. Ameghiniana 40 (2), 129–153.

956 Quattrocchio, M.E., Martínez, M.A., Hinojosa, L.F., Jaramillo, C., 2013. Quantitative
957 analysis of Cenozoic palynofloras from Patagonia (southern South America). Palynology
958 37 246-258. https://doi.org/10.1080/01916122.2013.787126

959 Quattrocchio, M.E., Olivera, D.E., Martınez, M.A., Ponce, J.J., Carmona, N.B., 2018.
960 Palynofacies associated to hyperpycnite deposits of the Miocene, Cabo Viamonte Beds,
961 Austral Basin, Argentina. Facies 64 (3), 1-14.

962 Quattrocchio, M.E., Martínez, M.A., Umazano, A.M., Tamame, M.A., Agüero, L., 2021.
963 The Danian Sea: Dinoflagellate cysts assemblages from Neuquén Basin, Roca Formation
964 (Argentina) and its comparison with other southern South America localities. J. South
965 Am. Earth Sci. 111, 103469. https://doi.org/10.1016/j.jsames.2021.103469

966 Röhl, U., Brinkhuis, H., Stickley, C.E., Fuller, M., Schellenberg, S.A., Wefer, G.,
967 Williams, G.L., 2004. Sea Level and Astronomically Induced Environmental Changes in
968 Middle and Late Eocene Sediments from the East Tasman Plateau, in: The Cenozoic
969 Southern Ocean: Tectonics, Sedimentation, and Climate Change Between Australia and
970 Antarctica. American Geophysical Union (AGU), pp. 127–151.
971 https://doi.org/10.1029/151GM09

972 Romero, E.J., 1986. Paleogene phytogeography and climatology of South America.
973 Annals of the Missouri Botanical Garden 73, 449–461.

974 Ronchi, D.I., Pérez Panera, J.P., Cuciniello, C.D., Ottone, E.G., 2015. Análisis
975 bioestratigráfico de muestras de afloramiento del Paleógeno de Tierra del Fuego:
976 Microfósiles, Nanofósiles calcáreos y Palinología. YPF Tecnología S.A. (Inédito).
977 Ensenada: Provincia de Buenos Aires p. 59.

978 Sageman, B.B., Lyons, T.W., 2004. Geochemistry of fine-grained sediments and
979 sedimentary rocks. In: MacKenzie, F. (Ed.), 2004. Sediments, Diagenesis, and
980 Sedimentary Rocks, Treatise on Geochemistry vol. 7, 115-158.

981 Salas, R. M., 2021. Sinopsis de Randia (Rubiaceae) de Bolivia. Boletín de la Sociedad
982 Argentina de Botánica 56, 575-598.

983 Shcherbinina, E., Gavrilov, Y., Iakovleva, A., Pokrovsky, B., Golovanova, O.,
984 Aleksandrova, G., 2016. Environmental dynamics during the Paleocene–Eocene thermal
985 maximum (PETM) in the northeastern PeriTethys revealed by high-resolution
986 micropalaeontological and geochemical studies of a Caucasian key section.
987 Palaeogeography, Palaeoclimatology, Palaeoecology 456, 60-81.

988 Schouten, S., Woltering, M., Rijpstra, W. I. C., Sluijs, A., Brinkhuis, H., Sinninghe
989 Damsté, J. S., 2007. The Paleocene-Eocene carbon isotope excursion in higher plant
990 organic matter: Differential fractionation of angiosperms and conifers in the Arctic. Earth
991 and Planetary Science Letters 258, 581–592.

992 SERNAGEOMIN, 2003. Mapa Geológico de Chile. Scale 1:1.000.000. Servicio Nacional
993 de Geología y Minería, Santiago.

994 Slimani, H., Mahboub, I., Toufiq, A., Jbari, H., Chakir, S., Tahiri, A., 2019. Bartonian to
995 Priabonian dinoflagellate cyst biostratigraphy and paleoenvironments of the M'karcha
996 section in the Southern Tethys margin (Rif Chain, Northern Morocco). Marine
997 Micropaleontology 153, 101785. https://doi.org/10.1016/j.marmicro.2019.101785

998 Sluijs, A., Brinkhuis, H., 2009. A dynamic climate and ecosystem state during the
999 Paleocene-Eocene Thermal Maximum: inferences from dinoflagellate cyst assemblages
1000 on the New Jersey Shelf. Biogeosciences 6, 1755–1781. https://doi.org/10.5194/bg-6-
1001 1755-2009

1002 Sluijs, A., Pross, J., Brinkhuis, H., 2005. From greenhouse to icehouse: organic-walled
1003 dinoflagellate cysts as paleoenvironmental indicators in the Paleogene. Earth-Science
1004 Reviews 68(3-4), 281–315.

1005 Sluijs, A., Brinkhuis, H., Crouch, E.M., John, C.M., Handley, L., Munsterman, D.,
1006 Bohaty, S.M., Zachos, J.C., Reichart, G.J., Schouten, S., Pancost, R.D., Sinninghe

1007 Damsté, J.S., Welters, N.L.D., Lotter, A.F., Dickens, G.R., 2008. Eustatic variations
1008 during the Paleocene-Eocene greenhouse world. Paleoceanography, 23, PA4216.
1009 https://doi:10.1029/2008PA001615

1010 Sluijs, A., Bijl, P.K., Schouten, S., Röhl, U., Reichart, G.J., Brinkhuis, H., 2011. Southern
1011 ocean warming, sea level and hydrological change during the Paleocene-Eocene thermal
1012 maximum. Climate of the Past 7, 47–61.

1013 Speijer, R.P., Wagner, T., 2002. Sea-level changes and black shales associated with the
1014 late Paleocene thermal maximum: Organic geochemical and micropaleontologic evidence
1015 from the southern Tethyan margin (Egypt-Israel). Geological Society of America Special
1016 Paper 356, 533–549.

1017 Steeman, T., De Weirdt, J., Smith, T., De Putter, T., Mees, F., Louwye, S., 2020.
1018 Dinoflagellate cyst biostratigraphy and palaeoecology of the early Paleogene Landana
1019 reference section, Cabinda Province, Angola. Palynology 44, 280–309.
1020 https://doi.org/10.1080/01916122.2019.1575091

1021 Suárez, M., de la Cruz, R., Troncoso, A., 2000. Tropical/subtropical Upper Paleocene-
1022 Lower Eocene fluvial deposits in eastern central Patagonia, Chile. Journal of South
1023 American Earth Sciences, 13, 527-536.

1024 Sun, Q., Daryin, A., Zhao, J., Xie, M., Darin, F., Rakshun, Y., 2021. High-resolution
1025 elemental record from the Holocene sediments of an alpine lake in the central Altai
1026 Mountains: Implications for Arctic sea-ice variations. Earth and Space Science, 8,
1027 e2021EA001810. https://doi.org/10.1029/2021EA001810

1028 Taylor, K.W.R., Willumsen, P.S., Hollis, C.J., Pancost, R.D., 2018. South Pacific
1029 evidence for the long-term climate impact of the Cretaceous/Paleogene boundary event.
1030 Earth-Science Reviews 179, 287–302. https://doi.org/10.1016/j.earscirev.2018.02.012

1031 Torres Carbonell, P.J., Malumian, N., Olivero, E.B., 2009. El Paleoceno-Mioceno de
1032 Peninsula Mitre: antefosa y depocentro de techo de cuna de la cuenca Austral, Tierra del
1033 Fuego, Argentina. Andean Geology 36 (2), 197–235.

1034 Torres Carbonell, P.J., Olivero, E.B., 2019. Tectonic control on the evolution of
1035 depositional systems in a fossil, marine foreland basin: Example from the SE Austral
1036 Basin, Tierra del Fuego, Argentina. Marine and Petroleum Geology 104, 40-60.

1037 Trappe, J., 1998. Phanerozoic phosphorite depositional systems. Lecture Notes in Earth
1038 Sciences 76.

1039 Traverse, A., 2007. Paleopalynology: Second Edition, 2nd ed, Topics in Geobiology.
1040 Springer Netherlands. https://doi.org/10.1007/978-1-4020-5610-9

1041 Tribovillard, N., Algeo, T.J., Lyons, T., Riboulleau, A., 2006. Trace metals as paleoredox
1042 and paleoproductivity proxies: An update. Chemical Geology, 232, 12-32.

1043 Tyson, R.V., 1995. Sedimentary Organic Matter. Springer Netherlands, Dordrecht.
1044 https://doi.org/10.1007/978-94-011-0739-6

1045 Van Mourik, C.A., Brinkhuis, H., Williams, G.L., 2001. Mid- to Late Eocene organic-
1046 walled dinoflagellate cysts from ODP Leg 171B, offshore Florida. Geological Society,
1047 London, Special Publications 183, 225–251.
1048 https://doi.org/10.1144/GSL.SP.2001.183.01.11

1049 Vellekoop, J., Smit, J., van de Schootbrugge, B., Weijers, J.W.H., Galeotti, S., Sinninghe
1050 Damsté, J.S., Brinkhuis, H., 2015. Palynological evidence for prolonged cooling along
1051 the Tunisian continental shelf following the K–Pg boundary impact. Palaeogeography,
1052 Palaeoclimatology, Palaeoecology 426, 216–228.
1053 https://doi.org/10.1016/j.palaeo.2015.03.021

1054 Volkheimer, W., Melendi, D., 1976. Palinomorfos como fosiles guías (3ra. Parte).
1055 Técnicas de laboratorio palinológico. Revista Minera, Geología y Mineralogía. Sociedad
1056 Argentina de Minería y Geología 34, 19–30.

1057 Wall, D., Dale, B., Lohmann, G.P., Smith, W.K., 1977. The environmental and climatic
1058 distribution of dinoflagellate cysts in modern marine sediments from regions in the North
1059 and South Atlantic Oceans and adjacent seas. Marine Micropaleontology 2, 121–200.
1060 https://doi.org/10.1016/0377-8398(77)90008-1

1061 Wilf, P., Johnson, K.R., Cuneo, R., Smith, E., Singer, B.S., Gandolfo, A., 2005. Eocene
1062 plant diversity at Laguna del Hunco and Rıo Pichileufu, Patagonia, Argentina. The
1063 American Naturalist 165, 634–650.

1064 Wilf, P., Little, S.A., Iglesias, A., Zamaloa, M.C., Gandolfo, M.A., Cuneo, N.R., Johnson,
1065 K.R., 2009. Papuacedrus (Cupressaceae) in Eocene Patagonia: a new fossil link to
1066 Australasian rainforests. American Journal of Botany 96, 2031–2047.

1067 Wilf, P., Cúneo, N.R., Escapa, I.H., Pol, D., Woodburne, M.O., 2013. Splendid and
1068 Seldom Isolated: The Paleobiogeography of Patagonia. Annual Review of Earth and
1069 Planetary Sciences 41, 561–603. https://doi.org/10.1146/annurev-earth-050212-124217

1070 Williams, G.L, Brinkhuis, H., Pearce, M.A., Fensome, R.A., Weegink, J.W., 2004.
1071 Southern Ocean and global dinoflagellate cyst events compared: Index events for the late
1072 Cretaceous-Neogene. In: Exon N., Kennett J.P. (Eds.). Proceedings of the Ocean Drilling
1073 Program, scientific results 189, 1–98.

1074 Williams, G.L., Fensome, R.A, MacRae, R.A., 2017. DINOFLAJ3. American
1075 Association of Stratigraphic Palynologists, Data Series no. 2.
1076 http://dinoflaj.smu.ca/dinoflaj3

1077 Wilpshaar, M., Leereveld, H., 1994. Palaeoenvironmental change in the Early Cretaceous
1078 Vocontian Basin (SE France) reflected by dinoflagellate cysts. Review of Palaeobotany
1079 and Palynology, Dino 5-5th International Conference on Modern and Fossil
1080 Dinoflagellates 84, 121–128. https://doi.org/10.1016/0034-6667(94)90046-9

1081 Wilson, G.J., 1984. New Zealand Late Jurassic to Eocene dinoflagellate biostratigraphy-
1082 a summary. Newsletters on Stratigraphy 13(2), 104–117.

1083 Wilson, G.J., 1988. Paleocene and Eocene dinoflagellate cysts from Waipawa, Hawkes
1084 Bay, New Zealand. New Zealand Geological Survey Paleontological Bulletin 57, 1-96.

1085 Woelders, L., Vellekoop, J., Kroon, D., Smit, J., Casadío, S., Prámparo, M.B., Dinarès-
1086 Turell, J., Peterse, F., Sluijs, A., Lenaerts, J.T.M., Speijer, R.P., 2017. Latest Cretaceous
1087 climatic and environmental change in the South Atlantic region. Paleoceanography 32,
1088 466–483. https://doi.org/10.1002/2016PA003007

1089 Woodburne, M.O., Goin, F.J., Raigemborn, M.S., Heizler, M., Gelfo, J.N., Oliveira, E.V.,
1090 2014. Revised timing of the South American early Paleogene land mammal ages. Journal
1091 of South American Earth Sciences 54, 109-119.

1092 Yabe, A., Uemura, K., Nishida, H., 2006. Geological notes on plant fossil localities of the
1093 Ligorio Márquez Formation, central Patagonia, Chile. In: Nishida H. (Ed.) Post-
1094 Cretaceous Floristic Changes in Southern Patagonia, Chile. Chuo. University Tokyo 29-
1095 35.

1096 Zavada, M.S., Benson, J.M., 1987. First fossil evidence for the primitive angiosperm
1097 family Lactoridaceae. American Journal of Botany 74, 1590–1594.

1098 Zavala, C., 2020. Hyperpycnal (over density) flows and deposits. Journal of
1099 Palaeogeography 9, 1-21.

1100

1101

1102

1103

1104

1105

1106

1107

1108

1109

1110

1111

1112

1113

1114

1115

1116

1117

1118

1119

FIGURE CAPTIONS

Figure 1. A. Regional map of southern South America (modified from Malumián et al., 2013) showing the location of Punta Prat and Punta Ainol sections and other localities in the Magallanes-Austral Basin. 1. B. Satellite image and geologic sketch of western Brunswick Peninsula, Chile, indicating the distribution of Chorrillo Chico and Agua Fresca formations and the location of the studied section at Punta Prat, compiled from SERNAGEOMIN (2003) and ENAP (1992). 1. C. Satellite image and geologic sketch of southeastern Tierra del Fuego, Argentina, indicating the location of the studied section of the La Barca Formation at Punta Ainol and the distributions of the Paleogene lithostratigraphic units: Cabo Leticia Formation (upper Paleocene), La Barca Formation (upper Paleocene-lower Eocene) including the distribution of LB1 and LB2 members in Cabo Leticia and Punta Ainol, Punta Noguera Formation (lower Eocene), Leticia Formation (middle Eocene) and Cerro Colorado Formation (upper Eocene), compiled mainly from Olivero et al. (2002), Torres Carbonell et al. (2009), Bedoya et al. (2018) and Torres Carbonell and Olivero (2019).

Figure 2. Stratigraphic section of the Chorrillo Chico and Agua Fresca formations from Punta Prat, Chile, indicating location of the samples, distribution of dinoflagellates cysts events, terrigenous input, type of depositional environment, geochemical parameters and chemozones. Ages according to the GTS2020 time scale of Gradstein and Ogg (2020).

Figure 3. Stratigraphic section of the La Barca Formation from Punta Ainol, Argentina, showing location of the palynological preparations, distribution of dinoflagellate cysts events, terrigenous input, type of depositional environment, geochemical parameters and chemozones. Ages according to the GTS2020 time scale of Gradstein and Ogg (2020).

Table 1. Distribution of palynomorphs recovered from the La Barca Formation at Punta Ainol section with their botanical affinities.

Table 2. Distribution of dinoflagellate cysts in the Chorrillo Chico and Agua Fresca formations, Punta Prat, Chile.

Table 3. Distribution of dinoflagellate cysts in the La Barca Formation at Punta Ainol, Tierra del Fuego.

Table 4. Paleoecological preferences of the identified dinoflagellate cysts ecogroups or taxa.

Plate I. Selection of dinoflagellate cysts considered in the palynostratigraphic analysis of the Chorrillo Chico, Agua Fresca (both at Punta Prat locality, figs. 1–8) and La Barca (Punta Ainol locality, figs. 9–14) formations. Scale bar = 10 μm.

1. *Achilleodinium biformoides* (Eisenack 1954) Eaton 1976 (Sample PP25).
2. *Eisenackia crassitabulata* Deflandre & Cookson 1955 (Sample PP25; Slide 3989/1; J32).
3. *Deflandrea cygniformis* Pöthe de Baldis 1966 (Sample PP10; Slide 3974/4; F39/2).
4. *Lejeunecysta fallax* Morgenroth 1966 (Sample PP20).
5. *Magallanesium macmurdoense* (Wilson 1967) Quattrocchio & Sarjeant 2003 (Sample PP9).
6. *Palaeoperidinium pyrophorum* (Ehrenberg 1838 ex Wetzel 1933) Sarjeant 1967 (Sample PP10; Slide 3974/5; F31/1).
7. *Pyxidinopsis delicata* Wilson 1988 (Sample PP22; Slide 3986/2; O44).
8. *Impagidinium cassiculum* Wilson 1988 (Sample PP13; Slide 3977/4; G36/4).
9. *Apectodinium homomorphum* (Deflandre & Cookson 1955) Lentin & Williams 1977 emend. Harland 1979 (Slide 4438a; P33).
10. *Cleistosphaeridium diversispinosum* Davey et al. 1966 emend. Eaton et al. 2001 (Slide 4440a; Q70/4).
11. *Enneadocysta dictyostila* (Menéndez) Fensome et al. 2006 (Slide 4452b; P70/1).

12. *Impagidinium crassimuratum* Wilson 1988 (Slide 4452b; H38).
13. *Pyxidinopsis waipawaensis* Wilson 1988 (Slide 4449a; D65/1).
14. *Samlandia septata* Wilson 1988 (*Slide 3121/2; T33). * From the La Barca Formation outcropping at Co. Malvinera (Quattrocchio, 2017).

Plate II. Selected sporomorphs from La Barca Formation, Punta Ainol locality. Scale bar = 10 μm.
1. *Cingutriletes australis* (Cook.) Archangelsky 1972 (Slide 4439a; J68/1).
2. *Biretisporites* sp. (Slide 4441b; L43/4).
3. *Cyathidites patagonicus* Archangelsky 1972 (Slide 4441a; S54).
4. *Trilites fasolae* Archangelsky 1972 (Slide 4445b; N72/3).
5-6. *Klukisporites* cf. *foveolatus* Pocock 1964 (Slide 4447a; F59).
7-8. *Camarozonosporites insignis* Harris 1967 (Slide 4450b; R36/2).
9-10. *Corrugatisporites argentinus* Archangelsky 1972 (Slide 4442b; T66).
11. *Hymenophyllumsporites* sp. (Slide 4441a; M22/2).
12. *Laevigatosporites ovatus* Wilson & Webster 1946 (Slide 4451b; F28/4).
13. *Podocarpidites elegans* Romero 1977 (Slide 4441b; H42).
14. *Gamerroites volkheimeri* Archangelsky 1988 (Slide 4445b; D43/3).
15. *Psilatricolpites* cf. *inargutus* (Mcintyre) Archangelsky 1973. (Slide 4438b; H44).
16. *Rhoipites cienaguensis* (Dueñas 1980) Barreda 1997 (Slide 4451b; J70/2).
17. *Nothofagidites kaitangataensis* (Te Punga) Romero 1973 (Slide 4440b; G39).
18. *Nothofagidites rocaensis* Romero 1973 (Slide 4446b; E36).
19. *Psilatricolporites salamanquensis* Archangelsky & Zamaloa 1986 (Slide 4450b; G72).
20. *Rosannia manika* (Srivastava) Srivastava & Braman 2010 (Slide 4443a; N71).
21. *Pandaniidites texus* Elsik 1968 (Slide 4440A; P26).
22. *Canthiumidites* aff. *C. bellus* (Partr.) Midl. & Pocock (in Barreda, 2002) (Slide 4440a; R47/4).
23. *Corsinipollenites atlantica* Barreda 1997 (Slide 4440a; S28/2).
24. *Proteacidites symphyonemoides* Cookson 1950 (Slide 4447a; Y62).

Table 1.

Fossil Taxon	Botanical affinity	Preparation Thickness (m)	4445 0	4444 19	4443 25	4442 32	4440 38	4441 44	4439 49	4438 55	4437 62	4449 71	4448 74	4447 82	4446 89	4454 96	4453 102	4452 108	4451 113	4450 120
Sporomorphs																				
Baculatisporites comaumensis (Cookson) Potonié, 1956	Hymnophyllaceae					x														x
Baculatisporites turbioensis Archangelsky, 1972	Osmundaceae					x										x			x	
Biretisporites crassilabratus Archangelsky, 1972	Schizaceae					x						x				x		x	x	x
Biretisporites sp.	Schizaceae							x												
Camarozonosporites insignis Harris, 1967	Lycopodiales																			x
Ceratosporites cf. *equalis* Cookson & Dettmann, 1958	Lycopodiaceae, Selaginellaceae (*Selaginella)*								x											
Cingutriletes australis (Cook.) Archangelsky, 1972	Sphagnaceae		x			x		x	x				x	x	x	x			x	x	x
Corrugatisporites argentinus Archangelsky, 1972	Schizaceae?					x							x	x		x	x	x	x	x
Cyathidites paleospora (Martin) Alley and Broadbridge, 1992	Cyatheaceae																			
Cyathidites patagonicus Archangelsky, 1972	Cyatheaceae / Matoniaceae?							x					x		x			x	x	
Deltoidospora australis (Couper) Pocock, 1970	Polypodiaceae / Cyatheaceae			x				x	x			x	x	x		x				
Dictyophyllidites cf. *mortoni* (de Jersey) Play. & Dett., 1956	Matoniaceae										x									
Dictyophyllidites sp.	Matoniaceae																			
Foveotriletes palaequetrus Partridge in Stover & Partridge, 1973	Lycopodiaceae: *Lycopodium australianum* -type																			x
Gleicheniidites senonicus Ross, 1949	Gleicheniaceae							x										x		
Gleichenidites sp. (in Archangelsky, 1972)	Gleicheniaceae														x					
Hymenophyllumsporites sp.	Hymenophyllaceae							x												
Klukisporites cf. *foveolatus* Pocock, 1964	Schizaceae													x						
Laevigatosporites ovatus Wilson y Webster, 1946	Blechnaceae																		x	

Table 1 continuation.

Fossil Taxon	Botanical affinity	Preparation Thickness (m)	44450	44419	44325	44232	44038	44144	43949	43855	43762	43671	43574	43482	43389	43296	43102	42908	42713	42520
Reticulatisporites sp.														x						
Retitriletes austroclavatidites (Cook.) Döring et al., l963	Lycopodiaceae		x			x		x	x		x			x	x					x
Trilites fasolae Archangelsky, 1972	Dicksoniaceae		x															x		
Gymnosperm pollen																				
Araucariacites australis Cookson, 1947	Araucariaceae							x	x		x		x	x					x	x
Dilwynites granulatus Harris, 1965	Araucariaceae																			
Dacrycarpites australiensis Cookson & Pike, 1953	Podocarpaceae																		x	
Gamerroites volkheimeri Archangelsky, 1988	Podocarpaceae		x					x						x	x					
Microcachryidites antarcticus Cookson, 1947	Podocarpaceae: *Microcachrys*								x		x				x					
Phyllocladidites mawsonii Cookson, 1947	Podocarpaceae		x	x	x	x	x		x		x	x	x	x				x		x
Podocarpidites elegans Romero, 1977	Podocarpaceae							x								x	x		x	
Podocarpidites marwickii Couper, 1953	Podocarpaceae		x	x	x							x		x	x		x	x		x
Podocarpidites verrucosus Volkheimer, 1972	Podocarpaceae													x						x
Podocarpidites spp.	Podocarpaceae								x			x					x		x	
Angiosperm pollen																				
Canthiumidites aff. *C. bellus* (Partr.) Midl. & Pocock (in Barreda, 2002)	Rubiaceae: *Randia*						x	x												
Corsinipollenites atlantica Barreda, 1997	Onagraceae						x								x			x		
Nothofagidites kaitangataensis (Te Punga) Romero, 1973	Nothofagaceae						x													
Nothofagidites fortispinulosus Menendez & Caccavari, 1975	Nothofagaceae		x			x		x	x	x	x						x	x		
Nothofagidites rocaensis Romero, 1973	Nothofagaceae						x						x	x	x			x	x	

Table 1 continuation.

Fossil Taxon	Botanical affinity	Preparation Thickness (m)	4445 0	4444 19	4443 25	4442 32	4440 38	4441 44	4439 49	4438 55	4437 62	4449 71	4448 74	4447 82	4446 89	4454 96	4453 102	4452 108	4451 113	4450 120
Nothofagidites saraensis Menendez & Caccavari, 1975	Nothofagaceae				x	x														
Nothofagidites spp.	Nothofagaceae						x		x	x							x		x	x
Pandanidites texus Elsik, 1968	Pandanaceae						x											x	x	
Peninsulapollis gillii Dett. & Jars., 1988	Proteaceae					x				x								x		
Proteacidites symphyonemoides Cookson, 1950	Proteaceae: cf. *symphionema*													x						
Proteacidites sp.1 *(* in Olivero *et al.*, 1998)	Proteaceae								x											
Proteacidites sp. (in Fasola, 1969)	Proteaceae																			
Psilatricolpites cf. *inargutus* (Mc Intyre) Archangelsky, 1973	?Violaceae									x										
Psilatricolporites salamanquensis Archangelsky & Zamaloa, 1986													x					x		x
Retitricolporites chubutensis Archangelsky, 1973	Vitaceae / Rutaceae										x									
Rhoipites cienaguensis (Dueñas 1980) Barreda, 1997																			x	
Rosannia manika (Srivastava) Srivastava & Braman, 2010	Lactoridaceae				x															x

Table 2. Distribution of dinoflagellate cysts in the Chorrillo Chico and Agua Fresca formations, Punta Prat, Chile.

Formation	Chorrillo Chico								Agua Fresca														
Sample	PP5	PP6	PP7	PP8	PP9	PP10	PP11	PP12	PP13	PP14	PP15	PP16	PP17	PP18	PP19	PP20	PP21	PP22	PP23	PP24	PP25	PP26	PP27
Thickness (m)	39.5	51	58	68	77	91.4	105	114	124	134	145	155	160	169	178	184	195	208	221	229	239	247	255
Taxon																							
P. golzowense	X	X		X	X	X	X			X				X	X				X		X	X	
P. pyrophorum	X		X		X	X	X																
E. crassitabulata	X				X								X								X	X	
S. granulatus	X			`																			
S. membranaceous	X						X			X										X	X		
?I. maculatum		X						X															
S. styloniferum		X				X					X												
I. bakeri		X					X			X	X	X								X			
L. bergmannii		X			X	X				X			X							X			X
S. ramosus		X			X	X			X	X		X					X	X		X			X
D. boloniensis			X								X		X										
T. tenuistriatum				X	X	X	X						X										
E. chilensis					X																		
P. crassimurata					X																X		
S. colemanii					X							X	X										
M. macmurdoense					X																		
S. argentinum						X																	
S. (H.) cryptovesiculatus						X				X		X	X									X	
D. cygniformis						X																	
O. azcaratei						X				X									X				
T. filosa						X																	
S. cornuta						X																	
H. tubiferum						X																	
V. lanterna						X				X													
C. fragile							X	X		X		X								X			
D. fuegiensis							X											X					
D. granulata							X			X	X												
G. cf. *retiintexta*							X			X		X	X				X	X	X	X			X
I. cassiculum									X														
O. erinaceum									X														
Apteodinium sp.										X													
I. crassimuratum										X		X		X								X	X
S. dilwynensis										X					X					X			
P. delicata											X							X		X	X	X	
D. menendezii												X											
G. delicata														X									
B. micropapillata													X										
D. antarctica														X									
L. fallax															X	X						X	
A. latispinosum																	X		X				
M. asymmetricum																		X	X				X
Chiropteridium sp.																			X				
A. distinctum																			X				
A. biformoides																				X	X		
A. senoniensis																					X		
Hystrichostrogylon sp.																					X		
Leujenecysta sp.																					X		
C. speciosum																						X	

Table 3. Distribution of dinoflagellate cysts in the La Barca Formation at Punta Ainol, Tierra del Fuego.

Preparation	4445	4444	4443	4442	4440	4441	4439	4438	4437	4449	4448	4447	4446	4454	4453	4452	4451	4450
Thickness (m)	0	19	25	32	38	44	49	55	62	71	74	82	89	96	102	108	113	120
Taxon																		
P. golzowense	X	X	X	X	X	X	X	X		X								
S. nephroides	X																	
S. styloniferum	X				X	X			X									
M. rallum									X									
E. circumtabulata		X	X			X	X			X	X	X	X			X	X	
D. phosphoritica			X		X													
D. fuegiensis			X		X											X		
M. asymmetricum			X	X	X				X									
L. bergmannii				X														
C. lumectum					X													
P. crassimurata					X													
E. crassitabulata						X			X							X		
O. puelcherrimum						X	X								X			
I. crassimuratum							X	X			X					X		
A. homomorphum							X	X	X									
B. micropapillata							X	X									X	
S. colemanii								X										
D. antarctica									X									
D. boloniensis									X	X								
I. cassiculum									X									
L. fallax										X								
P. waipawaensis										X								
S. septata										X								
C. fragile											X							
C. diversispinosum											X							
D. heterophycta											X					X		
E. dictyostila																X		
T. pelagica															X	X		

Table 4. Paleoecological preferences of the identified dinoflagellate cysts ecogroups or taxa.

Ecogroup	Taxa	Paleoecological preferences	References
Achilleodinium	*Achilleodinium* spp.	Inner neritic settings.	(Van Mourik et al., 2001).
Areoligera complex	*Areoligera senoniensis* *Chiropteridium* sp. *Glaphyrocysta* spp.	Nearshore, shallow marine environments with high energy. It also has affinity for low terrestrial input and normal salinity.	(Brinkhuis and Zachariasse, 1988; Sluijs et al., 2005; Vellekoop et al., 2015; Frieling and Sluijs, 2018).
Apectodinium	*Apectodinium homomorphum*	Normal marine conditions and low terrestrial input.	(Bijl et al., 2021; Frieling and Sluijs, 2018).
Apteodinium	*Apteodinium* sp.	Inner neritic, neritic (open shallow marine) settings.	(Wilpshaar and Leereveld, 1994; Peyrot, 2011; Guler et al., 2014).
Cassidium	*Cassidium fragile*	High terrestrial input?	(Bijl et al., 2021).
Cleistosphaeridium	*Cleistosphaeridium* spp.	Coastal, nearshore to outer neritic environments.	(Pross and Brinkhuis, 2005; Lamolda and Mao, 1999; Steeman et al., 2020).
Cordosphaeridium complex	*Thalassiphora pelagica* *Tityrosphaeridium* *Turbiosphaera filosa*	Open marine, neritic-outer neritic water masses.	(Downie et al., 1971; Brinkhuis, 1994; Powell et al., 1996; Frieling and Sluijs, 2018; Quattrocchio et al., 2021).
Enneadocysta	*Enneadocysta dictyostila*	Coastal settings and/or slightly more distal offshore, less eutrophic setting and warm water masses.	(Röhl et al., 2004; Pross and Brinkhuis, 2005).
Hystrichosphaeridium	*Hystrichosphaeridium tubiferum*	Coastal and inner neritic conditions.	(Woelders et al., 2017; Guler et al., 2019).
Impagidinium	*Impagidinium* spp. *?Impagidinium maculatum*	Oligotrophic water masses, oceanic enviroments.	(Brinkhuis et al., 1992; Brinkhuis, 1994; Dale, 1996; Sluijs et al., 2005; Pross and Brinkhuis, 2005 among others).
Isabelidinium	*Isabelidinium bakeri*	Inner neritic settings with high terrestrial input.	(Arai and Viviers, 2013; Castro and Carvalho, 2015; Steeman et al., 2020).
Oligosphaeridium	*Oligosphaeridium puelcherrimum*	Tolerant to reduced salinity, possibly reflecting middle shelf settings.	(Harris and Tocher, 2003; Prauss, 2012; Deaf et al., 2020).
Operculodinium complex	*Lingulodinium bergmannii* *Operculodinium* spp.	Restricted to open marine, neritic water masses.	(Wall et al., 1977; Powell et al., 1996).
Palaeocystodinium	*Palaeocystodinium golzowense*	High productivity.	(Eshet et al., 1994; Vellekoop et al., 2015; Quattrocchio et al., 2021).
Palaeoperidinium pyrophorum	*Palaeoperidinium pyrophorum*	Nutrient-rich waters masses. Acmes in neritic, shelf to upper slope settings.	(Askin, 1988; Taylor et al., 2018).
Proximal apical gonyaulacoid cysts (PAGC)	*Batiacasphaera micropapillata* *Eisenackia* spp.	Marine waters with reduced salinity and high terrestrial input.	(Frieling and Sluijs, 2018; Steeman et al., 2020).
Protoperidinioids	*Leujenecysta* spp. *Selenopemphix*	Inner neritic environments, high nutrients, and upwelling zones.	(Frieling and Sluijs, 2018; Slimani et al., 2019; Bijl et al., 2021).
Pyxidinopsis	*Pyxidiniopsis* spp.	Open marine settings.	(Dale, 1996; Crouch and Brinkhuis, 2005; Vellekoop et al., 2015; Taylor et al., 2018).
Samlandia	*Samlandia septata*	Coastal to middle shelf depositional settings.	(Crouch and Brinkhuis, 2005; Bijl et al., 2021).
Spiniferites complex	*Hystrichostrogylon* sp. *Spiniferella cornuta* *Spiniferites* spp.	Open marine neritic environments, outer neritic conditions or even oceanic settings.	(Sluijs et al., 2008 and references therein; Steeman et al., 2020).
*Senegalinium*complex	*Alterbidinium distinctum* *Cerodinium speciosum* *Deflandrea* spp. *Magallanesium* spp. *Senegalinium* *Spinidinium* spp. *Volkheimeridium*	Low salinity and high nutrients related to an increase in fresh-water runoff.	(Sluijs and Brinkhuis, 2009; Frieling and Sluijs, 2018; Guler et al., 2019).

Figure 1.

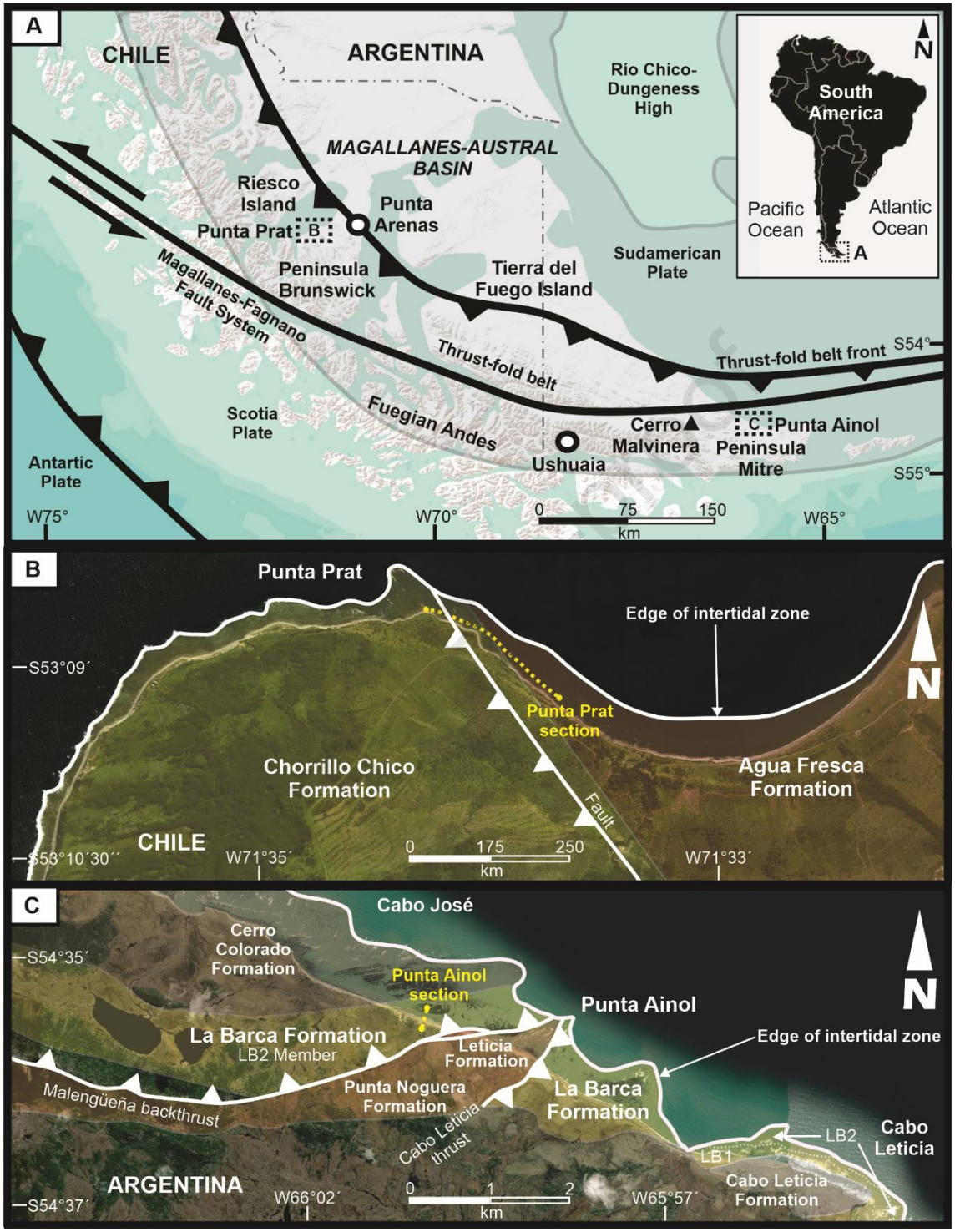
A
CHILE
ARGENTINA
Río Chico-
Dungeness
High
MAGALLANES-AUSTRAL
BASIN
Riesco
Island
Punta Prat
B
Punta
Arenas
Peninsula
Brunswick
Tierra del
Fuego Island
Sudamerican
Plate
Magallanes-Fagnano
Fault System
Thrust-fold belt
Thrust-fold belt front
S54°
Scotia
Plate
Fuegian Andes
Cerro
Malvinera
C
Punta Ainol
Peninsula
Mitre
Ushuaia
Antartic
Plate
S55°
W75°
W70°
0
75
150
km
W65°
N
South
America
Pacific
Ocean
Atlantic
Ocean
A
B
Punta Prat
Edge of intertidal zone
S53°09´
N
Punta Prat
section
Chorrillo Chico
Formation
Agua Fresca
Formation
Fault
CHILE
S53°10´30´´
W71°35´
0
175
250
km
W71°33´
C
Cabo José
Cerro
Colorado
Formation
S54°35´
Punta Ainol
section
Punta Ainol
N
La Barca Formation
LB2 Member
Leticia
Formation
Edge of intertidal zone
Malengüeña backthrust
Punta Noguera
Formation
La Barca
Formation
Cabo Leticia
thrust
LB2
Cabo
Leticia
LB1
ARGENTINA
S54°37´
W66°02´
0
1
2
km
W65°57´
Cabo Leticia
Formation

Figure 2.

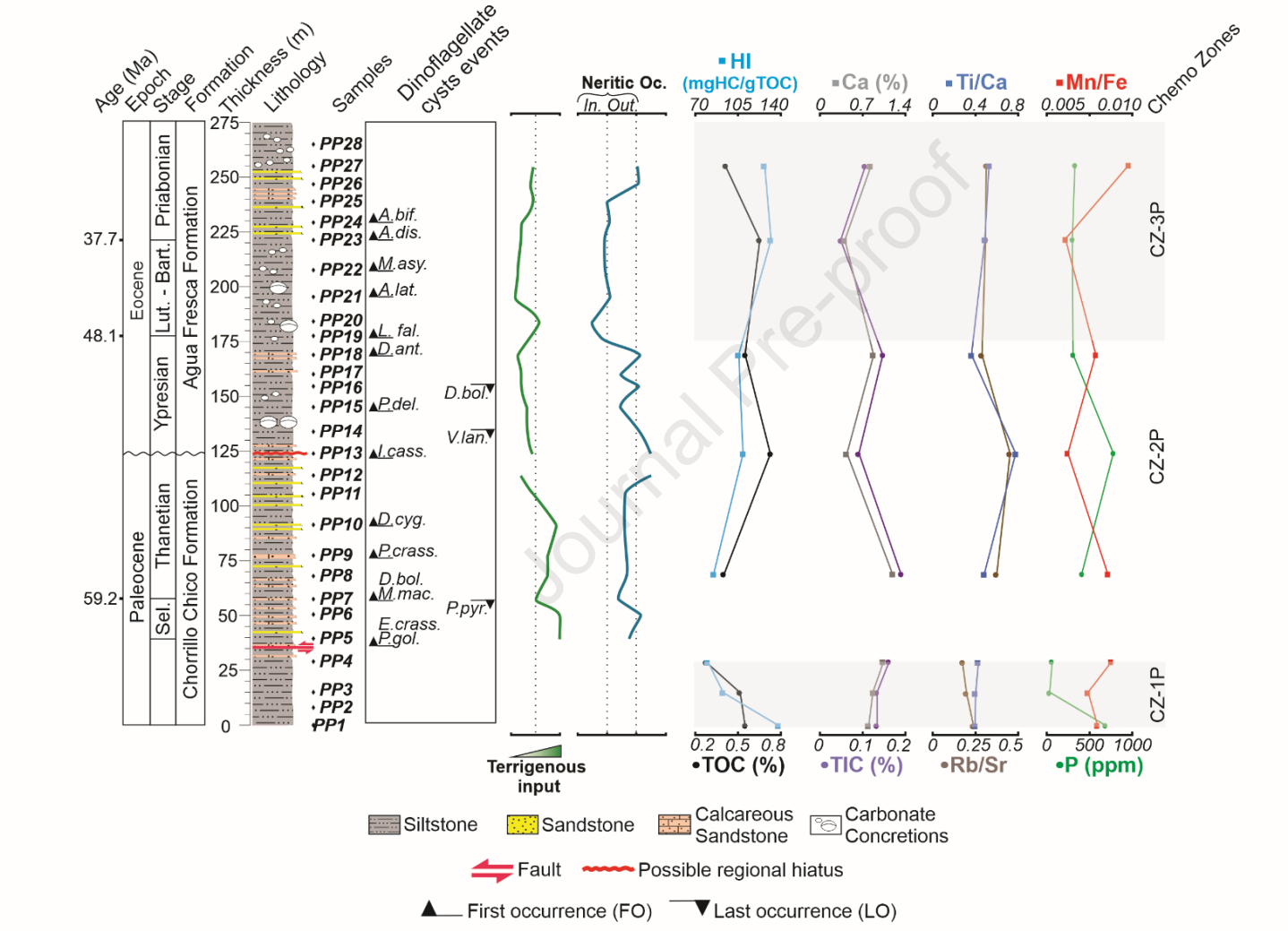

Figure 3.

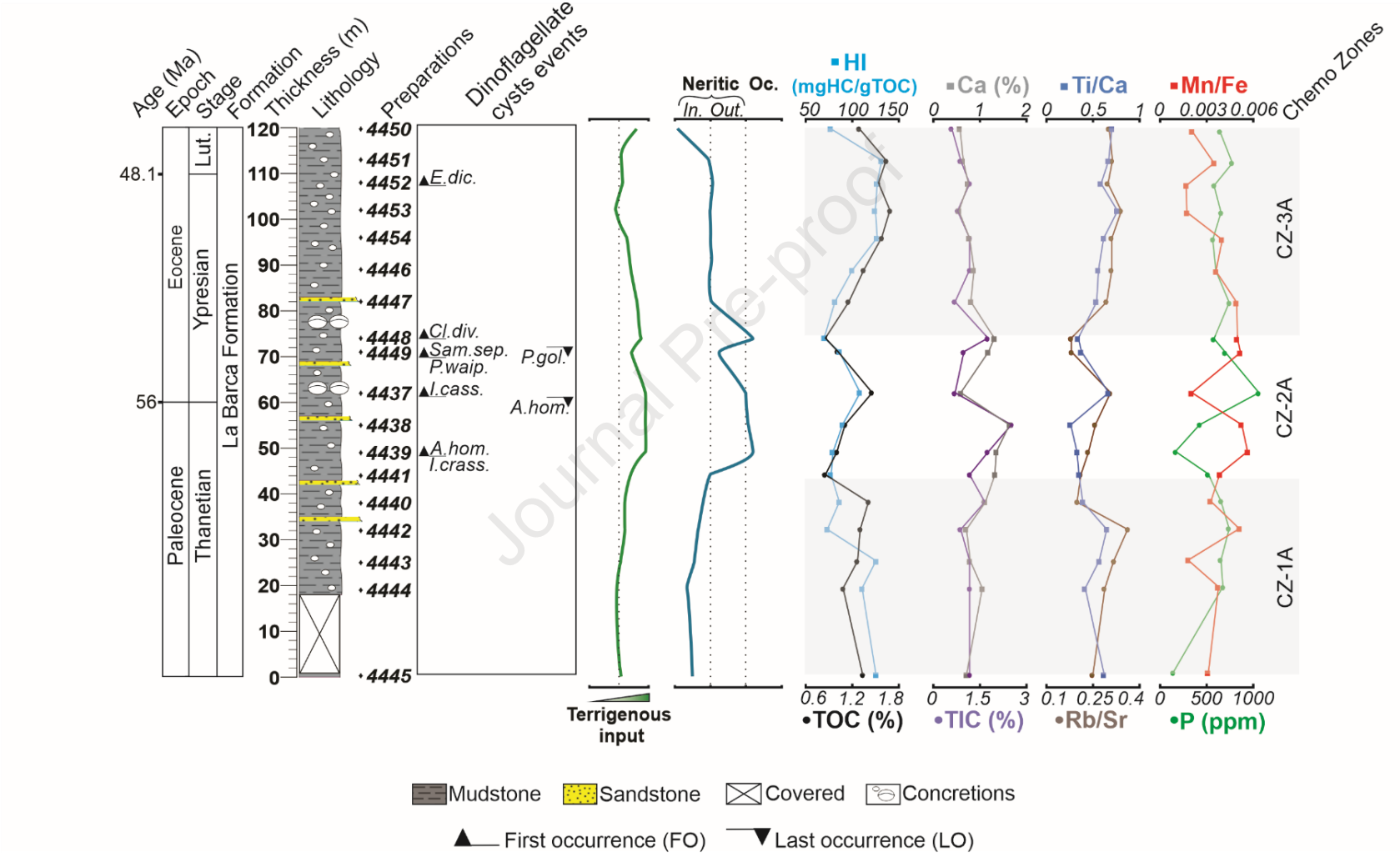
Age (Ma)
Epoch
Stage
Formation
Thickness (m)
Lithology
Preparations
Dinoflagellate cysts events
Neritic Oc.
In. Out.
HI (mgHC/gTOC)
Ca (%)
Ti/Ca
Mn/Fe
Chemo Zones
48.1
56
Eocene
Paleocene
Ypresian
Thanetian
Lut.
La Barca Formation
E.dic.
Cl.div.
Sam.sep.
P.waip.
P.gol.
I.cass.
A.hom.
A.hom.
I.crass.
Terrigenous input
TOC (%)
TIC (%)
Rb/Sr
P (ppm)
CZ-3A
CZ-2A
CZ-1A
Mudstone
Sandstone
Covered
Concretions
First occurrence (FO)
Last occurrence (LO)

Plate I.

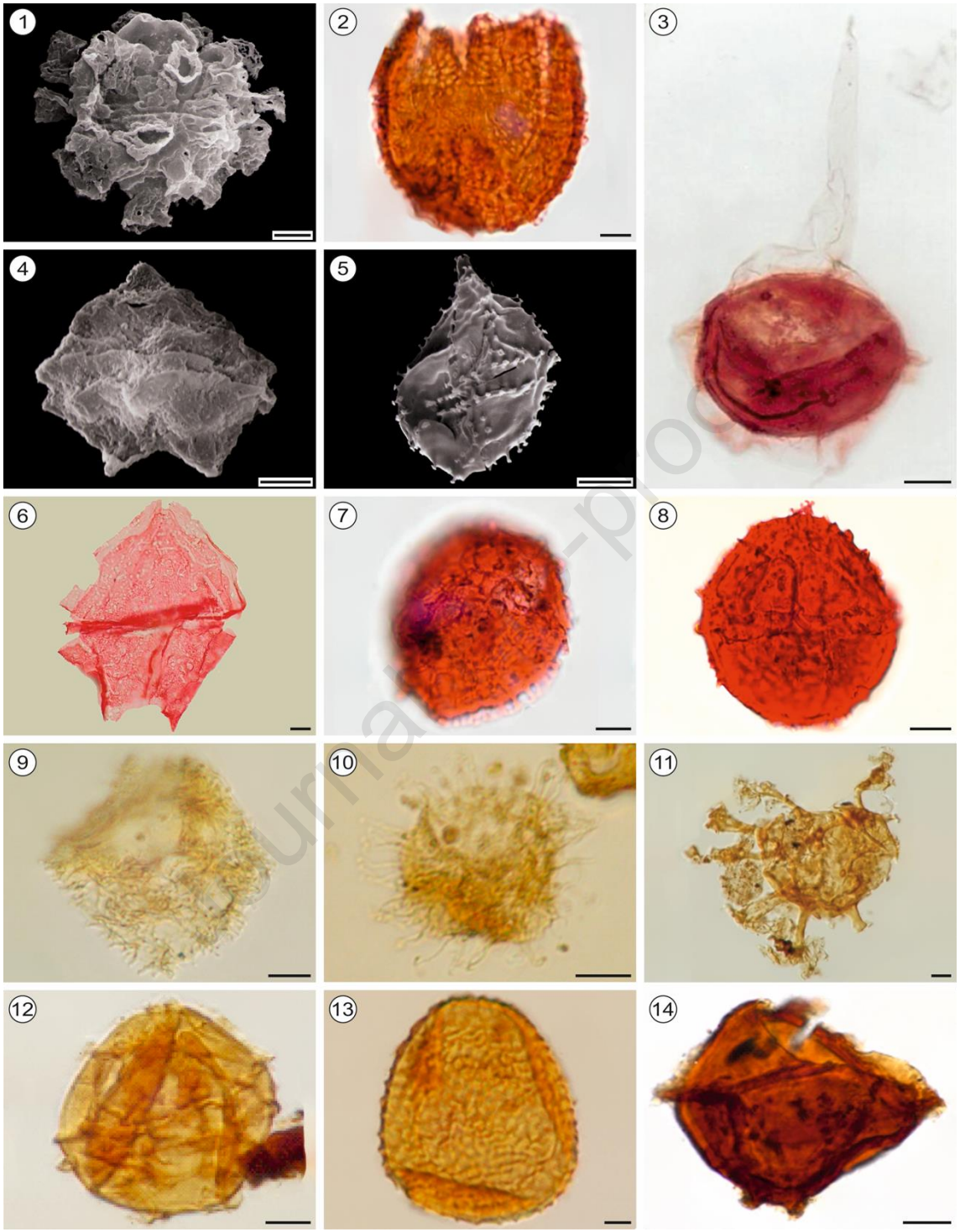

Plate II.

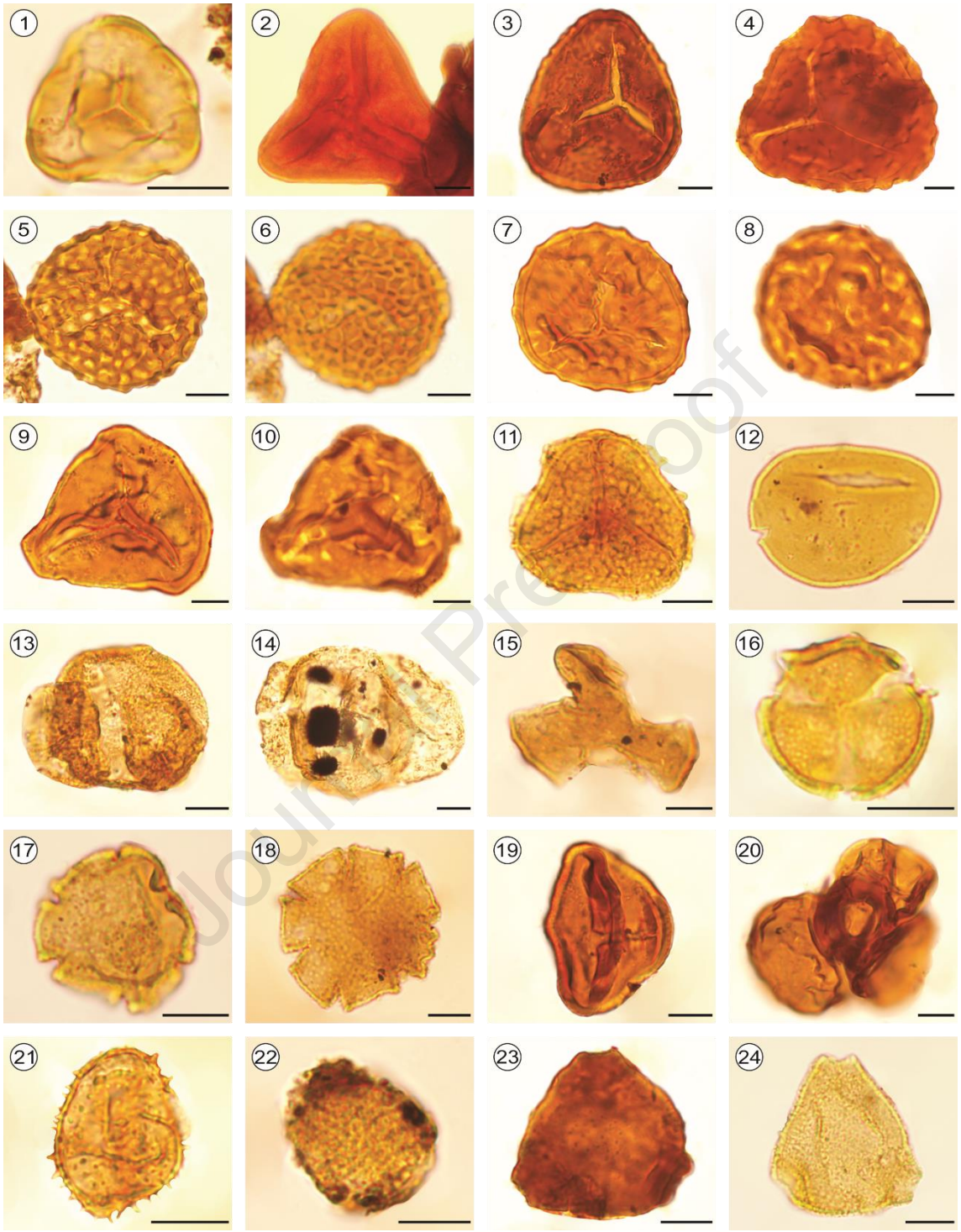

Table 4. Paleoecological preferences of the identified dinoflagellate cysts ecogroups or taxa.

Ecogroup	Taxa	Paleoecological preferences	References
Achilleodinium	*Achilleodinium* spp.	Inner neritic settings.	(Van Mourik et al., 2001).
Areoligera complex	*Areoligera senoniensis* *Chiropteridium* sp. *Glaphyrocysta* spp.	Nearshore, shallow marine environments with high energy. It also has affinity for low terrestrial input and normal salinity.	(Brinkhuis and Zachariasse, 1988; Sluijs et al., 2005; Vellekoop et al., 2015; Frieling and Sluijs, 2018).
Apectodinium	*Apectodinium homomorphum*	Normal marine conditions and low terrestrial input.	(Bijl et al., 2021; Frieling and Sluijs, 2018).
Apteodinium	*Apteodinium* sp.	Inner neritic, neritic (open shallow marine) settings.	(Wilpshaar and Leereveld, 1994; Peyrot, 2011; Guler et al., 2014).
Cassidium	*Cassidium fragile*	High terrestrial input?	(Bijl et al., 2021).
Cleistosphaeridium	*Cleistosphaeridium* spp.	Coastal, nearshore to outer neritic environments.	(Pross and Brinkhuis, 2005; Lamolda and Mao, 1999; Steeman et al., 2020).
Cordosphaeridium complex	*Thalassiphora pelagica* *Tityrosphaeridium* *Turbiosphaera filosa*	Open marine, neritic-outer neritic water masses.	(Downie et al., 1971; Brinkhuis, 1994; Powell et al., 1996; Frieling and Sluijs, 2018; Quattrocchio et al., 2021).
Enneadocysta	*Enneadocysta dictyostila*	Coastal settings and/or slightly more distal offshore, less eutrophic setting and warm water masses.	(Röhl et al., 2004; Pross and Brinkhuis, 2005).
Hystrichosphaeridium	*Hystrichosphaeridium tubiferum*	Coastal and inner neritic conditions.	(Woelders et al., 2017; Guler et al., 2019).
Impagidinium	*Impagidinium* spp. *?Impagidinium maculatum*	Oligotrophic water masses, oceanic enviroments.	(Brinkhuis et al., 1992; Brinkhuis, 1994; Dale, 1996; Sluijs et al., 2005; Pross and Brinkhuis, 2005 among others).
Isabelidinium	*Isabelidinium bakeri*	Inner neritic settings with high terrestrial input.	(Arai and Viviers, 2013; Castro and Carvalho, 2015; Steeman et al., 2020).
Oligosphaeridium	*Oligosphaeridium puelcherrimum*	Tolerant to reduced salinity, possibly reflecting middle shelf settings.	(Harris and Tocher, 2003; Prauss, 2012; Deaf et al., 2020).
Operculodinium complex	*Lingulodinium bergmannii* *Operculodinium* spp.	Restricted to open marine, neritic water masses.	(Wall et al., 1977; Powell et al., 1996).
Palaeocystodinium	*Palaeocystodinium golzowense*	High productivity.	(Eshet et al., 1994; Vellekoop et al., 2015; Quattrocchio et al., 2021).
Palaeoperidinium pyrophorum	*Palaeoperidinium pyrophorum*	Nutrient-rich waters masses. Acmes in neritic, shelf to upper slope settings.	(Askin, 1988; Taylor et al., 2018).
Proximal apical gonyaulacoid cysts (PAGC)	*Batiacasphaera micropapillata* *Eisenackia* spp.	Marine waters with reduced salinity and high terrestrial input.	(Frieling and Sluijs, 2018; Steeman et al., 2020).
Protoperidinioids	*Leujenecysta* spp. *Selenopemphix*	Inner neritic environments, high nutrients, and upwelling zones.	(Frieling and Sluijs, 2018; Slimani et al., 2019; Bijl et al., 2021).

Text-figure 3

Pyxidinopsis	*Pyxidiniopsis* spp.	Open marine settings.	(Dale, 1996; Crouch and Brinkhuis, 2005; Vellekoop et al., 2015; Taylor et al., 2018).
Samlandia	*Samlandia septata*	Coastal to middle shelf depositional settings.	(Crouch and Brinkhuis, 2005; Bijl et al., 2021).
Spiniferites complex	*Hystrichostrogylon* sp. *Spiniferella cornuta* *Spiniferites* spp.	Open marine neritic environments, outer neritic conditions or even oceanic settings.	(Sluijs et al., 2008 and references therein; Steeman et al., 2020).
Senegalinium complex	*Alterbidinium distinctum* *Cerodinium speciosum* *Deflandrea* spp. *Magallanesium* spp. *Senegalinium* *Spinidinium* spp. *Volkheimeridium*	Low salinity and high nutrients related to an increase in fresh-water runoff.	(Sluijs and Brinkhuis, 2009; Frieling and Sluijs, 2018; Guler et al., 2019).

Text-figure 3

Table 2. Distribution of dinoflagellate cysts in the Chorrillo Chico and Agua Fresca formations, Punta Prat, Chile.

Formation	Chorrillo Chico								Agua Fresca														
Sample	PP5	PP6	PP7	PP8	PP9	PP10	PP11	PP12	PP13	PP14	PP15	PP16	PP17	PP18	PP19	PP20	PP21	PP22	PP23	PP24	PP25	PP26	PP27
Thickness (m)	39.5	50.5	57.5	68	77.4	91.4	105	114	124	134	145	155	160	169	178	184	195	208	221	229	239	247	255
Taxon																							
P. golzowense	X	X		X	X	X	X			X				X	X				X		X	X	
P. pyrophorum	X		X		X	X	X																
E. crassitabulata	X				X								X								X	X	
S. granulatus	X			`																			
S. membranaceous	X						X			X										X	X		
?*I. maculatum*		X						X															
S. styloniferum		X				X					X												
I. bakeri		X					X			X	X	X								X			
L. bergmannii		X			X	X				X			X							X			X
S. ramosus		X			X	X			X	X		X					X	X		X			X
D. boloniensis			X								X		X										
T. tenuistriatum				X	X	X	X						X										
E. chilensis					X																		
P. crassimurata					X																X		
S. colemanii					X							X	X										
M. macmurdoense					X																		
S. argentinum						X																	
S. (H.) cryptovesiculatus						X				X		X	X									X	
D. cygniformis						X																	
O. azcaratei						X				X									X				
T. filosa						X																	
S. cornuta						X																	
H. tubiferum						X																	
V. lanterna						X				X													
C. fragile							X	X		X		X								X			
D. fuegiensis							X											X					
D. granulata							X			X	X												
G. cf. *retiintexta*							X			X		X	X				X	X	X	X			X
I. cassiculum									X														
O. erinaceum									X														
Apteodinium sp.										X													
I. crassimuratum										X		X		X								X	X
S. dilwynensis										X					X					X			
P. delicata											X							X		X	X	X	
D. menendezii												X											
G. delicata														X									
B. micropapillata													X										
D. antarctica														X									
L. fallax															X	X						X	
A. latispinosum																	X		X				
M. asymmetricum																		X	X				X
Chiropteridium sp.																			X				
A. distinctum																			X				
A. biformoides																				X	X		
A. senoniensis																					X		
Hystrichostrogylon sp.																					X		
Leujenecysta sp.																					X		
C. speciosum																						X	

Text-figure 3

Text-figure 3

Table 3. Distribution of dinoflagellate cysts in the La Barca Formation at Punta Ainol, Tierra del Fuego.

Preparation	4445	4444	4443	4442	4440	4441	4439	4438	4437	4449	4448	4447	4446	4454	4453	4452	4451	4450
Thickness (m)	0	19	25	32	38	44	49	55	62	71	74	82	89	96	102	108	113	120
Taxon																		
P. golzowense	X	X	X	X	X	X	X	X		X								
S. nephroides	X																	
S. styloniferum	X				X	X			X									
M. rallum									X									
E. circumtabulata		X	X			X	X			X	X	X	X			X	X	
D. phosphoritica			X		X													
D. fuegiensis			X		X											X		
M. asymmetricum			X	X	X				X									
L. bergmannii				X														
C. lumectum					X													
P. crassimurata					X													
E. crassitabulata						X			X							X		
O. puelcherrimum						X	X								X			
I. crassimuratum							X	X			X					X		
A. homomorphum							X	X	X									
B. micropapillata							X	X									X	
S. colemanii								X										
D. antarctica									X									
D. boloniensis									X	X								
I. cassiculum									X									
L. fallax										X								
P. waipawaensis										X								
S. septata										X								
C. fragile											X							
C. diversispinosum											X							
D. heterophycta											X					X		
E. dictyostila																X		
T. pelagica															X	X		

Text-figure 3

Fossil Taxon	Botanical affinity	Preparation Thickness (m)	4445 0	4444 19	4443 25	4442 32	4440 38	4441 44	4439 49	4438 55	4437 62	4449 71	4448 74	4447 82	4446 89	4454 96	4453 102	4452 108	4451 113	4450 120
Sporomorphs																				
Baculatisporites comaumensis (Cookson) Potonié, 1956	Hymnophyllaceae					**x**														**x**
Baculatisporites turbioensis Archangelsky, 1972	Osmundaceae					**x**										**x**			**x**	
Biretisporites crassilabratus Archangelsky, 1972	Schizaceae					**x**						**x**				**x**		**x**	**x**	**x**
Biretisporites sp.	Schizaceae							**x**												
Camarozonosporites insignis Harris, 1967	Lycopodiales																			**x**
Ceratosporites cf. *equalis* Cookson & Dettmann, 1958	Lycopodiaceae, Selaginellaceae (*Selaginella)*								**x**											
Cingutriletes australis (Cook.) Archangelsky, 1972	Sphagnaceae		**x**			**x**		**x**	**x**				**x**	**x**	**x**	**x**		**x**	**x**	**x**
Corrugatisporites argentinus Archangelsky, 1972	Schizaceae?					**x**							**x**	**x**		**x**	**x**	**x**	**x**	**x**
Cyathidites paleospora (Martin) Alley and Broadbridge, 1992	Cyatheaceae																			
Cyathidites patagonicus Archangelsky, 1972	Cyatheaceae/Matoniaceae?							**x**					**x**		**x**			**x**	**x**	
Deltoidospora australis (Couper) Pocock, 1970	Polypodiaceae / Cyatheaceae			**x**				**x**	**x**			**x**	**x**	**x**		**x**				
Dictyophyllidites cf. *mortoni* (de Jersey) Play. & Dett., 1956	Matoniaceae										**x**									
Dictyophyllidites sp.	Matoniaceae																			
Foveotriletes palaequetrus Partridge in Stover & Partridge, 1973	Lycopodiaceae: *Lycopodium australianum* -type																			**x**
Gleicheniidites senonicus Ross, 1949	Gleicheniaceae							**x**										**x**		
Gleichenidites sp. (in Archangelsky, 1972)	Gleicheniaceae														**x**					
Hymenophyllumsporites sp.	Hymenophyllaceae							**x**												

Klukisporites cf. *foveolatus* Pocock, 1964	Schizaceae													x					
Laevigatosporites ovatus Wilson y Webster, 1946	Blechnaceae																	x	

Fossil Taxon	Botanical affinity	Preparation Thickness (m)	4445 0	4444 19	4443 25	4442 32	4440 38	4441 44	4439 49	4438 55	4437 62	4449 71	4448 74	4447 82	4446 89	4454 96	4453 102	4452 108	4451 113	4450 120
Reticulatisporites sp.														x						
Retitriletes austroclavatidites (Cook.) Döring et al., l963	Lycopodiaceae		x			x		x	x		x			x	x					x
Trilites fasolae Archangelsky, 1972	Dicksoniaceae		x															x		
Gymnosperm pollen																				
Araucariacites australis Cookson, 1947	Araucariaceae							x	x		x		x	x					x	x
Dilwynites granulatus Harris, 1965	Araucariaceae																			
Dacrycarpites australiensis Cookson & Pike, 1953	Podocarpaceae																		x	
Gamerroites volkheimeri Archangelsky, 1988	Podocarpaceae		x					x						x	x					
Microcachryidites antarcticus Cookson, 1947	Podocarpaceae: *Microcachrys*								x		x				x					
Phyllocladidites mawsonii Cookson, 1947	Podocarpaceae		x	x	x	x	x		x		x	x	x	x				x		x
Podocarpidites elegans Romero, 1977	Podocarpaceae							x								x	x		x	
Podocarpidites marwickii Couper, 1953	Podocarpaceae		x	x	x							x		x	x		x	x		x
Podocarpidites verrucosus Volkheimer, 1972	Podocarpaceae													x						x
Podocarpidites spp.	Podocarpaceae								x			x					x		x	
Angiosperm pollen																				
Canthiumidites aff. *C. bellus* (Partr.) Midl. & Pocock (in Barreda, 2002)	Rubiaceae: *Randia*						x	x												
Corsinipollenites atlantica Barreda, 1997	Onagraceae						x								x			x		
Nothofagidites kaitangataensis (Te Punga) Romero, 1973	Nothofagaceae						x													

Nothofagidites fortispinulosus Menendez & Caccavari, 1975	Nothofagaceae			x			x			x	x	x	x						x	x
Nothofagidites rocaensis Romero, 1973	Nothofagaceae							x						x	x	x			x	x

Fossil Taxon	Botanical affinity	Preparation Thickness (m)	4445 0	4444 19	4443 25	4442 32	4440 38	4441 44	4439 49	4438 55	4437 62	4449 71	4448 74	4447 82	4446 89	4454 96	4453 102	4452 108	4451 113	4450 120
Nothofagidites saraensis Menendez & Caccavari, 1975	Nothofagaceae				x	x														
Nothofagidites spp.	Nothofagaceae						x		x	x							x		x	x
Pandanidites texus Elsik, 1968	Pandanaceae						x											x	x	
Peninsulapollis gillii Dett. & Jars., 1988	Proteaceae					x				x								x		
Proteacidites symphyonemoides Cookson, 1950	Proteaceae: cf. *symphionema*													x						
Proteacidites sp.1 *(* in Olivero *et al.,* 1998)	Proteaceae								x											
Proteacidites sp. (in Fasola, 1969)	Proteaceae																			
Psilatricolpites cf. *inargutus* (Mc Intyre) Archangelsky, 1973	?Violaceae									x										
Psilatricolporites salamanquensis Archangelsky & Zamaloa, 1986													x					x		x
Retitricolporites chubutensis Archangelsky, 1973	Vitaceae / Rutaceae										x									
Rhoipites cienaguensis (Dueñas 1980) Barreda, 1997																			x	
Rosannia manika (Srivastava) Srivastava & Braman, 2010	Lactoridaceae				x															x

Highlights

- A new register of early Paleogene flora of Patagonia.
- Paleogeographic changes based on palynological and geochemical data.
- New geochemical inferences of the Paleocene-Eocene transition in South America.
- A new Paleocene-Eocene record from Southern Hemisphere.

Declaration of interests

☒ The authors declare that they have no known competing financial interests or personal relationships that could have appeared to influence the work reported in this paper.

☐ The authors declare the following financial interests/personal relationships which may be considered as potential competing interests: